

The Dynamics of Two Interacting Giant Gravitons

Katherine Laura Elizabeth Ann Jefferies

April 2011

A dissertation submitted to the Faculty of Science, University
of the Witwatersrand, Johannesburg in fulfillment of the
requirements of the degree of Master of Science.

Declaration

I declare that this dissertation is my own, unaided work. It is submitted for the Degree of Master of Science in the University of the Witwatersrand, Johannesburg. It has not been submitted before for any degree or examination in any other University.

----- (Signature of candidate)

----- day of ----- 20-----

Abstract

In this thesis, the large N limit of the anomalous dimension of operators in $\mathcal{N} = 4$ super Yang-Mills theory described by restricted Schur Polynomials are studied. The operators studied in this thesis are labelled by Young Diagrams which have two columns (both long) so that the classical dimension of these operators is $O(N)$. At large N these two column operators mix with each other but are decoupled from operators with $n \neq 2$ columns. The planar approximation does not capture the large N dynamics. The dilatation operator is explicitly evaluated for 2, 3, and 4 impurities. In all three cases, for a certain limit, the dilatation operator is a discretized version of the second derivative defined on a lattice emerging from the Young Diagram itself. The dilatation operator is diagonalized numerically. All eigenvalues are an integer multiple of $8g_{YM}^2$ and there are interesting degeneracies in the spectrum. The spectrum obtained in this thesis for the one loop anomalous dimension operator is reproduced by a collection of harmonic oscillators. The equivalence to harmonic oscillators generalizes giant graviton results known for the BPS sector and further implies that the Hamiltonian defined by the one loop large N dilatation operator is integrable. This is an example of an integrable dilatation operator, obtained by summing both the planar and the non-planar diagrams.

Acknowledgments

I would like to thank my supervisor, Robert de Mello Koch for his patience and encouragement. I am very grateful for the numerous hours and the he invested in me.

I would also like to thank my mom, dad and sister Suzanne for their constant support and good humour.

I would also like to thank my fellow colleagues for all the insightful conversations and ideas.

Contents

1	Introduction	1
2	AdS/CFT correspondence	6
2.1	A brief history	6
2.2	Anti deSitter Space	8
2.3	Conformal Field Theory	10
2.4	Matching Parameters	14
3	Giant Gravitons	15
3.1	A brief review of an electric dipole moving in a magnetic field	16
3.2	$\text{AdS}_5 \times \text{S}^5$	17
4	Matrix Models and Schur Polynomials	25
4.1	Matrix Models	25
4.2	Schur Polynomials	31
4.2.1	Schur Polynomials- Unrestricted	32
4.2.2	Schur Polynomials- Restricted	36
5	Action of the Dilatation Operator	47
6	Excited Giant Graviton Bound States	51

7	The Radial Direction	53
7.1	Three Impurities	53
7.2	Four Impurities	57
8	Numerical Results	61
8.1	Two Impurities	61
8.2	Three Impurities	62
8.3	Four Impurities	62
9	Discussion	64
9.1	Results Discussion	64
9.2	Further Studies	68
A	Dilatation Operator for Three or Four Impurities	70
A.1	Three Impurities	70
A.2	Four Impurities	74
B	Intertwiners	80

List of Figures

4.1	The propagator for $\langle X_{ab}(x)X_{cd}(y) \rangle$	28
4.2	The propagator for $\langle X_{ab}(x)X_{ba}(x) \rangle$	28
4.3	$\langle Tr(X^2)Tr(X^2) \rangle$	29
4.4	$\langle Tr(X^4) \rangle$	30
4.5	A Young Diagram with the weight of each block displayed . .	33
4.6	A Young Diagram with the hook length displayed in each box	35
4.7	Representation R	39
4.8	R'_1, R'_2, R'_3 respectively	39

Chapter 1

Introduction

In the last few years, interesting progress has been made in the study of the dynamics of multimatrix models. It was observed in [1] that Schur Polynomials are a complete basis of gauge invariant operators which diagonalize the two point function of the free ($g_{YM}^2 = 0$) super Yang- Mills Theory. Similar bases have been found for multimatrix models in [2, 3, 4, 5, 6, 7, 8, 9, 10, 11, 12]. The two point function for these bases is diagonal and known exactly as a function of N where $g_{YM}^2 = 0$.

As the N dependence is known exactly, it suggests that the results may be used for going beyond the planar limit. It must be noted that “the planar limit” and “the large N limit” are, in general, not the same concept. To see this, suppose one computes the two point correlator of an operator with a bare dimension Δ of most $\Delta \sim J$ with $\frac{J^2}{N} \ll 1$. Summing the planar diagrams will capture the large N limit. If one were to consider an operator with dimensions larger than this, then the combinatoric factors will overpower the nonplanar ($\frac{1}{N^2}$) suppression and the planar approximation is completely ineffective[13]. In this case, it is necessary to sum more than the planar diagrams in order to get the correct large N limit. In general, one expects

the large N limit to be simpler than the full theory [14]. As the planar diagrams represent a small subset of all possible diagrams, it is natural to expect the summation of these diagrams to provide a simpler problem. But why should one expect the large N limit to be simple when one sums more than the planar diagrams? The answer to this may not be general and may depend on the specific dynamical problem considered and might be answered case by case. One approach may be to consider the large N limit and simply look for simplifications. This was accomplished in [15, 16, 17] in a number of examples including LLM geometries [18, 19] and the near horizon geometry of a bound state of giant gravitons [20]. The results obtained are surprisingly simple. As an example, for $\frac{1}{2}$ BPS- correlators in the presence of M giant gravitons with M of order N , [15, 16, 17] showed that the usual $\frac{1}{N}$ expansion was replaced by a $\frac{1}{M+N}$ expansion. As these correlators are $\frac{1}{2}$ BPS (they do not depend on g_{YM}^2 but only on N and M), then the expansion coefficients for the correlators in the background of M giants are the same as the expansion coefficients for correlators with no giants present. This simple result was confirmed holographically in [21] by matching to graviton dynamics in the LLM geometries using the formalism of [22]. For near BPS operators corresponding to BMN loops [23] it was argued in [24, 25, 26] that the usual 't Hooft coupling $g_{YM}^2 N$ is replaced by the effective 't Hooft coupling $g_{YM}^2 (N + M)$.

In this thesis, the problem of computing the one loop anomalous dimension of an operator with a bare dimension of order N will be considered. In order to examine this, we explore beyond the planar limit using the methods and approach of [2, 3, 4, 5, 6, 7, 8, 9, 10, 11]. The results obtained are rather simple- the spectrum of the anomalous dimension can be matched to the spectrum of a set of oscillators. Once again, it is seen that the large N

limit is a simple limit. This result is obtained by considering restricted Schur Polynomials as the operators used, built using $O(N)$ Z s and 3 or 4 “impurities” (Y s) where Z and Y are the complex adjoint scalars of $\mathcal{N}=4$ super Yang Mills theory. The case of operators with two impurities was studied in [30]. When the dilatation operator acts on a restricted Schur Polynomial, it produces terms that have a $ZY - YZ$ combination. In [30], the techniques of [4, 6] were used to separate the Z and the Y and write the results as a linear combination of restricted Schur Polynomials. This calculation becomes cumbersome as it involves the inversion of a matrix. For the two impurities case, the matrix that is inverted is 6×6 and must be done analytically. Any case with more impurities seemed out of reach following this method. In this thesis, a new formula is developed which avoids the matrix inversion. This can be seen in Chapter 5. Using the new formula, the case for three and four impurities can be handled without much trouble. As can be seen in Appendix A, the expressions obtained for the action of the dilatation operator are long and complicated however, the spectrum obtained is quite simple. The results suggest that for the class of operators considered, the Hamiltonian defined by the dilatation operator is integrable as it is just a set of oscillators. This is an example of an integrable dilatation operator obtained from summing both the planar and the non-planar diagrams. The operators considered in this thesis can be mapped to giant gravitons [28] in spacetime [13, 1, 29]. There is already a known connection between the geometry of giant gravitons and harmonic oscillators [31, 32, 33, 34, 35, 36]. Although this is the case, the work presented in this thesis differs from the previous work in two very important ways. Firstly, we claim that the complete spectrum, not just the BPS spectrum, has a connection to harmonic oscillators. Secondly, we have control over the set of operators used as they are dual to

the two giant system. Previous studies captured the full set of BPS states and consequently were not able to distinguish, for example, giant graviton with graviton from excited giant gravitons. In this thesis, only the states of the two giant system are captured. Thus it is possible to associate the oscillators with excitation modes of a giant graviton.

The restricted Schur Polynomials studied in this thesis are built by distributing “impurities” (Ys) in an operator built mainly from Zs . By replacing the Ys by words containing $O(\sqrt{N})$ letters; which could be Z , Y , other fields or derivatives of fields, these words are naturally identified with open strings [37, 38, 39]. In this case the dilatation operator reproduces the dynamics of open strings connected to a giant graviton [40, 3, 4, 6]. The mixing of operators is highly constrained. It was shown in [4, 6] that operators which mix can differ at most by moving one box around on the Young Diagram labeling the operator. Another interesting basis to consider is the Brauer basis [5, 11]. This basis is built using Brauer algebra projectors. The structure constants of the Brauer algebra are N dependent. There is an elegant construction of a class of BPS operators [41] in which the natural N dependence appearing in the definition of the operator [42] is naturally reproduced by the Brauer algebra projectors[41]. Another approach to this problem is to adopt a basis with sharp quantum numbers for the global symmetries of the theory [7, 9]. The action of the anomalous dimension operator in this basis is very similar to the action on the restricted Schur basis. Operators which mix can differ at most by moving one box around on the Young diagram labeling the operator [43]. For a general approach for counting and constructing the weak coupling BPS operators, see [36].

This thesis is organized as follows: Chapter Two will give a brief review of the AdS/CFT correspondence. Chapter Three will be a review of the

paper *Invasion of the giant graviton from anti – de Sitter space* by J. McGreevy, L. Susskind and N. Toumbas [30]. Chapter Four will give a brief review of Matrix Models as well as on Schur Polynomials (the operators dual in conformal field theory to giant gravitons). Chapters Five to Chapter Eight will be on the research done and the results obtained. Chapter Nine will give a summary of the results and a conclusion to this thesis. The results of this thesis have been reported in arXiv:1012.3884v1[hep-th] and have been submitted to JHEP for publication.

Chapter 2

AdS/CFT correspondence

In this chapter, a brief review of the AdS/CFT correspondence shall be given. This will include a brief history as to why this correspondence is studied as well as what exactly the AdS space is and what a Conformal Field Theory is and why they are dual to each other.

2.1 A brief history

For many decades, physicists have worked hard at the problem of trying to unify the four fundamental forces of nature- the electromagnetic force, the strong force, the weak nuclear force and gravity. The study of quantum mechanics and Einstein's general theory of relativity have provided descriptions of physics at both the subatomic scale and the cosmological scale. Quantum mechanics has successfully been combined with the electromagnetic force and the weak nuclear force to give the electroweak force, the theory of which is a quantum field theory. The combination of quantum mechanics with special relativity in a quantum field theory gives rise to quantum chromodynamics (QCD). The Standard Model is composed of the electroweak theory and

QCD. A theory which combines both quantum mechanics and the force of gravity (quantum gravity), however, has not yet been found. It is believed that string theory holds the answer to this unifying puzzle.

String theory is a theory which describes elementary particles as loops of string, not much bigger than the Planck scale. These strings are one-dimensional and each oscillation mode of a string corresponds to a different particle in perturbative string theory. By assuming these strings are one dimensional has the result that supersymmetric theories must be built using 10 dimensions to be consistent. These extra dimensions of space are said to be compactified so as to ensure that one is left with a 3+1 dimensional world. One might think that the inclusion of extra dimensions into a theory in order for it to work would automatically count it as wrong however this is not the case. Present in this theory is a massless spin two boson which can only be associated with a gravity carrying particle-a graviton. The particle arises out of the theory, it was not put in by hand. This makes string theory a viable option for quantum gravity [51].

There are several different types of string theory, each of which can be formulated using different backgrounds. The type studied in this thesis is that of IIB string theory whose background is composed of a five dimensional non compact Anti deSitter (*AdS*) space and a five sphere (S^5) as it is a solution to the IIB supergravity equations of motion. According to the Maldacena's conjecture [52], the quantum string that lives on the AdS_5 background is dual to the conformally invariant field theory living on a 4 dimensional spacetime, which is interpreted as the boundary of the AdS space. This conformally invariant field theory is the maximally supersymmetric $SU(N)$ Yang Mills theory in 4 dimensional Minkowski space. It is known as "maximally supersymmetric" as it has the most supersymmetry for a theory that contains no

gravity. It is known as a conformal field theory because it is invariant under conformal transformations (to be discussed later)[55]. Maldacena’s conjecture is a realization of the holographic principle initially proposed by Gerard ’t Hooft [53] and later extended by Leonard Susskind [54]. The holographic principle states that the physical description of quantum gravity in a volume of space is encoded in an ordinary quantum field theory (QFT) living on the boundary of the space. This is most easily imagined using a regular hologram, usually a two dimensional object which gives rise to a three dimensional image.

It must be noted that the AdS/CFT correspondence is a correspondence between two theories, one which contains gravity (AdS) and one which does not contain gravity (CFT). It must also be mentioned that the word “dual” means the full equivalence between the two theories. Each side of the correspondence shall now be briefly discussed. For the mathematical details, it is suggested that one consider [55, 56].

2.2 Anti deSitter Space

As previously mentioned, the AdS side of the correspondence forms part of the background of the type IIB string theory. Through the space flows the IIB 5- form flux which is an integer multiple of N . The equal radii of the AdS₅ space and the S⁵ space is given by $R^4 = 4\pi g_s N l_s^4$ where g_s is the string coupling and l_s is the string length. (This will be seen again in chapter three).

An Anti deSitter space, itself, is a space with constant negative curvature. To picture this, one could think of a saddle where the curvature at every point along the saddle is the same. AdS space is a solution to the Einstein equations with a negative cosmological constant. This can be shown simply

using AdS_5 space. The AdS_5 space can be described as the hypersurface

$$R^2 = x_0^2 + x_5^2 - x_1^2 - x_2^2 - x_3^2 - x_4^2$$

in a six-dimensional space such that the metric for the space is given by

$$ds^2 = -dx_0^2 - dx_5^2 + dx_1^2 + dx_2^2 + dx_3^2 + dx_4^2$$

Consider the following parametrization

$$\begin{aligned} X_0 &= \frac{1}{2u}(1 + u^2(\vec{x} \cdot \vec{x} - t^2) + u^2 R^2) \\ X_4 &= \frac{1}{2u}(1 + u^2(\vec{x} \cdot \vec{x} - t^2) - u^2 R^2) \\ X_i &= Rux^i \\ X_5 &= Rut \end{aligned} \tag{2.1}$$

where $i = 1, 2, 3$. Before continuing, it must be noted that this parameterization of the surface which does not cover the entire surface, is called a Poincaré patch. To see this, note that for $u > 0$, one always has $X_0 > X_4$. This means that the $X_0 < X_4$ part of AdS_5 has not been captured. Using this parametrization, the metric can be rewritten as follows

$$ds^2 = R^2 \left(u^2(-dt^2 + d\vec{x} \cdot d\vec{x}) + \frac{du^2}{u^2} \right) \tag{2.2}$$

From the analysis of this metric, it can be seen that there is a horizon at $u=0$. When $u \rightarrow \infty$, then one is at a boundary. Setting $u = \frac{1}{z}$ results in the metric

$$ds^2 = \frac{1}{z^2}(-dt^2 + d\vec{x} \cdot d\vec{x} + dz^2) \tag{2.3}$$

The curvature of the space can be calculated. This is done by calculating the Christoffel symbols. Once these have been calculated, the Riemann curvature tensor can be calculated which will then be used to obtain the Ricci tensor.

The result shall be stated here without the calculations shown. The result obtained for the Ricci tensor is

$$R_{\mu\nu} = -4g_{\mu\nu} \quad (2.4)$$

where $g_{\mu\nu}$ is defined as in equation (2.3). In terms of the cosmological constant, the Ricci tensor (applicable to AdS_d) is given by

$$\begin{aligned} R_{\mu\nu} &= \Lambda g_{\mu\nu} \\ R_{\mu\nu} &= -(d-1)g_{\mu\nu} \end{aligned} \quad (2.5)$$

and $R=-(d-1)d$ so for AdS_5 , $R=-20$.

In summary, the AdS_5 surface was parameterized by a set of co-ordinates which did not cover the entire space. In metric (2.2) when $u=0$, a horizon is obtained and when $u \rightarrow \infty$ a boundary is obtained. The co-ordinate $z = \frac{1}{u}$ was also considered. When the limit of $z \rightarrow \infty$ is taken, it is seen that the metric goes to zero and it the one is in the middle of the AdS space. When the limit $z=0$ is taken, it can be seen that one is at the boundary of the entire AdS space. This solution can be thought of as putting the Universe in a box. Indeed, geodesics leave the origin and return exactly as if the particle was in a harmonic oscillator potential.

2.3 Conformal Field Theory

A conformal field theory (CFT) is defined as being a quantum field theory (QFT) that is invariant under conformal transformations. A conformal transformation is a transformation which scales the metric (angles are preserved). Suppose one has the following change of co-ordinates

$$x \rightarrow x'$$

then the metric will change as follows

$$g_{\mu\nu}(x) \rightarrow g'_{\mu\nu}(x') = \Omega(x)g_{\mu\nu}(x)$$

where $\Omega(x)$ gives the information for how the metric has been scaled.

There are many different types of conformal transformations, each with their own $\Omega(x)$. These conformal transformations are Lorentz rotations, translations, dilatations and special conformal transformations. Each conformal transformation has its own generator.

For Lorentz boosts and rotations, $\Omega(x)$ is set to one. This is not surprising as the action of boosting an object or rotating it does not change its proper length. In this case, the generator for these transformations is given by

$$M_{\mu\nu} = i(x_\mu\partial_\nu - x_\nu\partial_\mu)$$

For translations, $\Omega(x)$ is again one. Again, this is not surprising as the action of changing one's position does not change its length. The generator in this case is

$$P_\mu = i\partial_\mu$$

In cases where the metric does not change, one is said to have an isometry.

For dilatations, the metric scaling factor is not one. Consider the following transformation

$$x^\mu \rightarrow \lambda x^\mu$$

where λ is a constant. From this transformation, the metric scaling factor can be obtained.

$$\begin{aligned} ds^2 &= g_{\mu\nu}dx^\mu dx^\nu \\ &= \frac{g_{\mu\nu}}{\lambda^2}d(\lambda x^\mu)d(\lambda x^\nu) \\ &= \frac{g_{\mu\nu}}{\lambda^2}dx'^\mu dx'^\nu \end{aligned} \tag{2.6}$$

From equation(2.6) it can be seen that

$$\Omega = \lambda^{-2} \tag{2.7}$$

In order to obtain the generator of dilatations, one needs to consider the infinitesimal transformation

$$x^\mu \rightarrow (1 + \epsilon)x^\mu \tag{2.8}$$

By considering equation (2.8) alone, the generator for the dilatation is not obvious. It is however if one considers the following

$$\begin{aligned} x^\mu &\rightarrow (1 + \epsilon)^\mu x^\mu \\ &= (1 + \mu\epsilon)x^\mu \end{aligned}$$

From this transformation, it can be seen that the generator is

$$D = -ix^\mu \partial_\mu$$

This just counts the number of x^μ 's.

For special conformal transformations, the metric scaling factor is, again not one. Consider the following transformation

$$x^\mu \rightarrow \frac{x^\mu + a^\mu x^2}{1 + 2a \cdot x + a^2 x^2}$$

where a^μ is any four vector.

For this transformation, the metric scaling factor is given by

$$\Omega = (1 + 2a \cdot x + a^2 x^2)^2 \tag{2.9}$$

In order to find the generator of this transformation, the infinitesimal transformation must be considered. To do this, substitute a with ϵ and expand

$$x^\mu \rightarrow x^\mu + \epsilon^\mu x^2 - 2\epsilon \cdot x x^\mu$$

Thus the generator is given by

$$K_\mu = i(x^2 \partial_\mu - 2x_\mu x^\nu \partial_\nu)$$

In order to test any theory, one must ask what is observable. In quantum field theory, the observable is the S-matrix. The S-matrix allows the observer to consider a non interacting system in the past, allows the system to interact and then compare the non interacting system in the future to ascertain what happened during the interaction. In CFTs, the S-matrix is not an observable. This is because in a CFT, the concept of the distant past and far future has no meaning as a scaling in time is a symmetry. An observable in CFT is the scaling dimension or the anomalous dimension. The anomalous dimension is a function related to the shift in the field strength as a result of renormalisation. The standard method for obtaining the anomalous dimension Δ_α is to consider the two point function of a set of conformal fields $\hat{\mathcal{O}}_\alpha$ [45]

$$\langle \hat{\mathcal{O}}_\alpha(x) \hat{\mathcal{O}}_\beta(y) \rangle = \frac{\delta_{\alpha\beta}}{|x-y|^{2\Delta_\alpha}}$$

The eigensystem of the dilatation operator, \hat{D} is composed of the eigenstates $\hat{\mathcal{O}}_\alpha$ and the eigenvalues Δ_α [45]

$$\hat{D} \hat{\mathcal{O}}_\alpha = \Delta_\alpha \hat{\mathcal{O}}_\alpha$$

In this thesis, the $\mathcal{N} = 4$ SYM field theory is considered. We will study the action of the one loop dilatation operator on a restricted Schur Polynomial. The one loop dilatation operator in the SU(2) sector [45] of the $\mathcal{N} = 4$ super Yang-Mills Theory is

$$D = -g_{YM}^2 \text{Tr}[Y, Z][\partial_Y, \partial_Z]$$

where g_{YM}^2 is the Yang Mills coupling.

2.4 Matching Parameters

Going back to Maldacena's conjecture, there is a relationship between the string coupling g_s and the Yang Mills coupling g_{YM} as follows

$$g_{YM}^2 = g_s$$

Substituting in for the string coupling gives

$$Ng_{YM}^2 = \frac{R^4}{l_s^4} \tag{2.10}$$

If one now takes the limit $N \rightarrow \infty$ while holding Ng_{YM}^2 large and fixed, one can see that $\frac{R^4}{l_s^4}$ is big and thus one would expect that this limit of the gauge theory is dual to a weakly coupled gravity theory on a smooth spacetime.

Chapter 3

Giant Gravitons

In this chapter, the paper *Invasion of the giant gravitons from anti-de Sitter space* by J. McGreevy, L.Susskind and N.Toumbas [28] will be reviewed. In this paper, the physical origin of the stringy exclusion principle is examined and is shown to be the result of a large distance phenomenon. The stringy exclusion principle is a limit on the number of single particle states propagating on the spherical component of $AdS_n \times S^m$. The particles considered in this paper are gravitons or any other massless particles in S^m . The paper argues that the particles are dipoles. This implies that there is no net charge but they expand when set in motion. When the size of the particle reaches the radius of the space, the particle can no longer grow in size. This implies a bound on the angular momentum which reproduces the stringy exclusion principle. In order to show this, the authors review the theory of electric dipoles moving in a magnetic field as a non-commutative field theory. The authors then consider the motion of a massless particle in three different maximally supersymmetric spaces: $AdS_7 \times S^4$, $AdS_4 \times S^7$ and $AdS_5 \times S^5$. A brief review of the section on dipoles will be given as well as the motion of a massless particle on $AdS_5 \times S^5$.

3.1 A brief review of an electric dipole moving in a magnetic field

In this section, the motion of an electric dipole moving in a uniform magnetic field is considered. The dipole is composed of a pair of oppositely charged unit charges. The dipole has some kinetic energy and experiences a force as a result of the applied uniform magnetic field (Lorentz Force). There is also a force present between the two unit charges which is like that of a Hooke force. It is assumed that the mass of the unit charges, and consequently the dipole, is small such that the kinetic energy of the dipole can be ignored in comparison to the effects from the magnetic field and the force between the unit charges. By considering the relative co-ordinates and the centre of mass co-ordinates of the dipole, it is found that the co-ordinates are non-commuting variables. From further analysis it is also seen that the dipole is stretched as it moves in a direction perpendicular to the applied field with some momentum. This is a basis for non-commutative field theory with non-local effects. In order to learn more about the motion of the dipole, it is assumed that the dipole is moving on the surface of a sphere with some magnetic flux. Making this assumption implies that there is a magnetic monopole at the centre of the sphere. By parameterising the sphere and analyzing the Lagrangian density obtained for the electric dipole, a key result is obtained. It was found that the angular momentum of the dipole in the non-commutative field is bounded by the magnetic flux on the sphere and that it is a long distance effect. This means that as momentum of the dipole increases, so does its size. The faster the dipole orbits the surface of the sphere, the larger the dipole gets until it reaches the size of the sphere and dipole can no longer grow. Thus the dipole's motion is limited by some

maximum momentum.

3.2 $\text{AdS}_5 \times \text{S}^5$

Here the motion of a BPS particle on a five-sphere is considered. The assumption will be made that the radius of curvature of the space R is much greater than the ten dimensional Planck length l_p . The motion of the BPS particle is considered as it moves through a five-form field strength on the sphere. The flux density is labelled B . The quantization of flux requires

$$\Omega_5 B R^5 = 2\pi N \quad (3.1)$$

where R is the radius of the S^5 space and is given by

$$R = (4\pi g_s N)^{\frac{1}{4}} l_s \quad (3.2)$$

where g_s is the string coupling constant, N is the number of units of flux on the sphere and l_s is the string length. As it was assumed that R is much larger than l_s then N must be large with $g_s N$ both large and fixed.

In order to obtain the relationship between N and the angular momentum L of the graviton, it is necessary to consider the motion of the graviton on the five-sphere in a five-form field strength. Substituting (3.2) into (3.1) and dropping the constants gives an expression for B in terms of N

$$B \approx N^{-\frac{1}{4}} l_s^{-5} g_s^{-\frac{5}{4}} \quad (3.3)$$

With our conventions, B fills the $(x^5, x^6, x^7, x^8, x^9)$ directions. The graviton will move in the x^9 direction with momentum

$$P_9 = \frac{L}{R} \quad (3.4)$$

This is the usual form of the momentum in terms of angular momentum.

Parametrize S^5 using Cartesian co-ordinates X_1, \dots, X_6 as follows

$$\begin{aligned}
X_1 &= R \cos \theta_1 \\
X_2 &= R \sin \theta_1 \cos \theta_2 \\
X_3 &= R \sin \theta_1 \sin \theta_2 \cos \theta_3 \\
X_4 &= R \sin \theta_1 \sin \theta_2 \sin \theta_3 \cos \theta_4 \\
X_5 &= R \sin \theta_1 \sin \theta_2 \sin \theta_3 \sin \theta_4 \cos \theta_5 \\
X_6 &= R \sin \theta_1 \sin \theta_2 \sin \theta_3 \sin \theta_4 \sin \theta_5
\end{aligned} \tag{3.5}$$

where $\theta_1, \dots, \theta_4$ range from 0 to π and θ_5 is the azimuthal angle ranging from 0 to 2π . This correctly describes the five-sphere

$$X_1^2 + X_2^2 + X_3^2 + X_4^2 + X_5^2 + X_6^2 = R^2 \tag{3.6}$$

We consider a spherical membrane embedded in S^5 . Any angles can be chosen to parametrize the worldvolume of this membrane. Here, the choice is made to parametrize the worldvolume of the membrane using $\theta_3, \theta_4, \theta_5$. This means that the brane will move in the transverse X_1, X_2 plane. The size of the membrane depends on where it is on the X_1, X_2 plane according to

$$r_5 = R \sin \theta_1 \sin \theta_2 \tag{3.7}$$

Clearly the size of the membrane is at a maximum when $\theta_1 = \theta_2 = \frac{\pi}{2}$ resulting in $r_5 = R$. Making this substitution back into the parametrization of the membrane, one obtains $X_1 = X_2 = 0$ which means that the membrane, at its maximum size, is at the origin. Using the $r_5 = R$ relationship results in

$$R^2 - r_5^2 = X_1^2 + X_2^2 \tag{3.8}$$

From this, it can be seen that the membrane can move around in a circle in the plane with a constant size. As a result of this the following expressions for X_1 and X_2 can be obtained

$$\begin{aligned} X_1 &= \sqrt{R^2 - r_5^2} \cos \phi \\ X_2 &= \sqrt{R^2 - r_5^2} \sin \phi \end{aligned} \quad (3.9)$$

This means that the original parametrization of the five-sphere as seen in equation (3.5) can be rewritten as

$$\begin{aligned} X_1 &= \sqrt{R^2 - r_5^2} \cos \phi \\ X_2 &= \sqrt{R^2 - r_5^2} \sin \phi \\ X_3 &= r_5 \cos \theta_3 \\ X_4 &= r_5 \sin \theta_3 \cos \theta_4 \\ X_5 &= r_5 \sin \theta_3 \sin \theta_4 \cos \theta_5 \\ X_6 &= r_5 \sin \theta_3 \sin \theta_4 \sin \theta_5 \end{aligned} \quad (3.10)$$

Using these co-ordinates, the metric on the five- sphere can be rewritten in terms of $r_5, \phi, \theta_3, \theta_4, \theta_5$

$$ds^2 = \frac{R}{R^2 - r_5^2} dr_5^2 + (R^2 - r_5^2) d\phi^2 + r_5^2 d\Omega_3^2 \quad (3.11)$$

where $d\Omega_3$ is the solid angle of the three sphere parametrized by θ_3, θ_4 and θ_5 . It can be seen that the volume element is

$$Rr_5^2 dr_5 d\phi d\Omega_3 \quad (3.12)$$

The metric on the worldvolume of the membrane needs to still be calculated. To do this, note that the complete spacetime metric is

$$ds^2 = ds_{AdS_5}^2 + ds_{S_5}^2 \quad (3.13)$$

The metric for the AdS space must still be included. In a convenient set of co-ordinates [48]

$$ds^2_{AdS_m} = -\left(1 + \frac{r^2}{L^2}\right)dt^2 + \frac{dr^2}{\left(1 + \frac{r^2}{L^2}\right)} + r^2 d\Omega_{m-2}^2 \quad (3.14)$$

When $m=5$

$$ds^2_{AdS_5} = -\left(1 + \frac{r^2}{L^2}\right)dt^2 + \frac{dr^2}{\left(1 + \frac{r^2}{L^2}\right)} + r^2 d\Omega_3^2 \quad (3.15)$$

For the purpose of this problem, $r=0$. Recall, it was stated earlier that the motion of the BPS particle on S_5 was to be considered as the membrane sits at the origin of the AdS_5 space. The radius r is the radial co-ordinate of AdS_5 and bears no relation to the one seen previously (r_5). Thus

$$ds^2_{worldvolume} = -dt^2 + \frac{R}{R^2 - r_5^2} dr_5^2 + (R^2 - r_5^2) d\phi^2 + r_5^2 d\Omega_3^2 \quad (3.16)$$

The parameters for the worldvolume are $d\theta_3$, $d\theta_4$, $d\theta_5$ and $d\tau$ where $t=\tau$.

As S_3 wraps in S_5 then r_5 is a constant so $dr_5=0$. The metric for the worldvolume thus becomes

$$ds^2 = -d\tau^2 + (R^2 - r_5^2) \dot{\phi}^2 d\tau^2 + r_5^2 d\Omega_3^2 = -(1 - (R^2 - r_5^2) \dot{\phi}^2) d\tau^2 + r_5^2 d\Omega_3^2 \quad (3.17)$$

From the definition of the metric, this can be written in general as

$$ds^2 = h_{ab} dx^a dx^b$$

where

$$h_{ab} = \begin{bmatrix} -(1 - (R^2 - r_5^2) \dot{\phi}^2) & 0 & 0 & 0 \\ 0 & r_5^2 & 0 & 0 \\ 0 & 0 & r_5^2 \sin^2 \theta_3 & 0 \\ 0 & 0 & 0 & r_5^2 \sin^2 \theta_3 \sin^2 \theta_4 \end{bmatrix} \quad (3.18)$$

Using this it is possible to obtain the kinetic energy of the membrane using the Dirac-Born-Infeld (DBI) Lagrangian. The DBI action is considered as the Lagrangian is easily read off of it.

The DBI action is given by[48]

$$S_{DBI} = \int -T_{m-2} \sqrt{-g} d\tau d\sigma_1 \dots d\sigma_{m-2} \quad (3.19)$$

where T is the tension of the brane and $\sqrt{-g}$ is the square root of the determinant of the metric.

Written for the system considered here:

$$S_{DBI} = \int -T_{D3} \sqrt{-h} d\tau d\theta_3 d\theta_4 d\theta_5 \quad (3.20)$$

where T_{D3} is the tension of the D3 brane wrapping S_5 and $\sqrt{-h}$ is the square root of the determinant of the matrix obtained in equation (3.18).

Substituting (3.18) into (3.20) gives

$$S_{DBI} = \int -T_{D3} \sqrt{1 - (R^2 - r_5^2) \dot{\phi}^2} r_5^3 d\tau d\Omega_3 \quad (3.21)$$

The kinetic component of the Lagrangian is now easily read from (3.21)

$$\mathcal{L}_K = -T_{D3} \Omega_3 r_5^3 \sqrt{1 - (R^2 - r_5^2) \dot{\phi}^2} \quad (3.22)$$

The tension of the D3 brane is given by

$$T_{D3} = \frac{1}{(2\pi)^3 l_s^4 g_s} \quad (3.23)$$

Using equation (3.2), (3.23) can be re-written in terms of N and R

$$T_{D3} = \frac{N}{\Omega_3 R^4} \quad (3.24)$$

and so the following expression is obtained

$$T_{D3} \Omega_3 = \frac{N}{R^4} \quad (3.25)$$

The kinetic contribution to the Lagrangian has been obtained. It is now necessary to obtain the contribution from the background field. In order to obtain this contribution, the Chern-Simons coupling involving the background field must be derived. The background field is the applied five-form field whose flux was denoted as B . The contribution of the five-form field strength to the action of the brane around S_5 is

$$S_B = \int_{wv} C = \int_{\Sigma} F \quad (3.26)$$

where the first integral is over the worldvolume of the brane. The second integral is over a five-manifold in S^5 whose boundary is a 4-dimensional surface swept out by the brane during an orbit. F is the background flux given by

$$F = B dVol$$

where B is the flux density and $dVol$ is the volume form of S_5 . The Chern-Simons action is

$$S_B = B Vol(\Sigma) \quad (3.27)$$

The contribution to the Lagrangian is thus given by

$$\mathcal{L}_B = \frac{S_B}{T} \quad (3.28)$$

where T is the period of the D3-brane motion. Equation (3.28) can be rewritten as follows

$$\mathcal{L}_B = B Vol(\Sigma) \frac{\dot{\phi}}{2\pi} \quad (3.29)$$

where $\dot{\phi}$ is the constant angular velocity of the brane. The volume of Σ is given by

$$Vol(\Sigma) = R \int_0^{r_5} r^3 dr \int_0^{2\pi} d\phi \int d\Omega_3 \quad (3.30)$$

Calculating the integral gives

$$Vol(\Sigma) = r_5^4 R \Omega_5 \quad (3.31)$$

Using equations (3.31) and (3.1), equation (3.29) can be rewritten as

$$\mathcal{L}_B = \dot{\phi} N \frac{r_5^4}{R^4} \quad (3.32)$$

The full Lagrangian for the system is thus given by

$$\begin{aligned} \mathcal{L} &= -T_{D3} \Omega_3 r_5^3 \sqrt{1 - (R^2 - r_5^2) \dot{\phi}^2} + \dot{\phi} N \frac{r_5^4}{R^4} \\ &= -m \sqrt{1 - (R^2 - r_5^2) \dot{\phi}^2} + \dot{\phi} N \frac{r_5^4}{R^4} \end{aligned} \quad (3.33)$$

where $m = T \Omega_3 r_5^3$.

In order to obtain the relationship between the angular momentum of the brane, L , and the number of units of flux of the sphere, N ; the angular momentum of the brane needs to be calculated from the Lagrangian. The expression for the angular momentum of the brane is

$$L = \frac{m(R^2 - r_5^2) \dot{\phi}^2}{\sqrt{1 - (R^2 - r_5^2) \dot{\phi}^2}} + \frac{N r_5^4}{R^4} \quad (3.34)$$

It is known that (see (3.10)) the size of the membrane cannot exceed R (the size of the S_5 space) and that the velocity of the brane cannot exceed the speed of light. Thus L is bounded by N .

If the membrane was the size of the space ($r_5 = R$) then it can be seen from (3.34) that

$$L_{max} = N \quad (3.35)$$

The maximum value for the angular momentum is N . When $r_5 \ll R$, then the brane is a Kaluza-Klein graviton which is free to increase in size as its angular momentum increases. However, when $r_5 = R$ then the Kaluza-Klein graviton has maximum angular momentum which agrees with the stringy exclusion principle. When $r_5 = R$, the membrane is at its maximal size in the S^5 space and is called a sphere giant graviton.

Using the Lagrangian for the system, the energy of the membrane can also be obtained

$$E = \dot{\phi}L - \mathcal{L} = \sqrt{m^2 + \frac{(L - \frac{Nr_5^4}{R^4})^2}{(R^2 - r_5^2)}} \quad (3.36)$$

In keeping L fixed and varying r_5 , the potential of the system can be obtained

$$\frac{dE}{dr_5} = \frac{r_5}{E(R^2 - r_5^2)^2} \left(L - \frac{3Nr_5^2}{R^2} + \frac{2Nr_5^4}{R^4} \right) \left(L - \frac{Nr_5^2}{R^2} \right) \quad (3.37)$$

When considering the minima from (3.38), there is a stable minimum at

$$r_5^2 = R^2 \frac{L}{N} \quad (3.38)$$

when $L < N$.

From finding the minima of the potential, it can be seen that the membrane does indeed increase in size as the angular momentum increases. Substituting this minimum into the expression obtained in (3.36) for the energy gives

$$E = \frac{L}{R} \quad (3.39)$$

This expression for the energy at the minimum is not surprising as it is what one would expect for a massless particle

$$\begin{aligned} E^2 &= \vec{p} \cdot \vec{p} - m^2 = p^2 \\ \Rightarrow E &= |\vec{p}| \\ &= \frac{L}{R} \end{aligned}$$

where L is the angular momentum of the brane and R is the size of the space.

Chapter 4

Matrix Models and Schur Polynomials

4.1 Matrix Models

As previously mentioned, the $\mathcal{N} = 4$ super Yang-Mills (SYM) theory is considered in this thesis. In chapter two, it was mentioned that this theory is a quantum field theory where the fields are matrix fields built from the complex linear combination of six scalar fields [1]. These matrix fields are

$$\begin{aligned} Z &= \Phi_1 + i\Phi_2 \\ Y &= \Phi_3 + i\Phi_4 \\ X &= \Phi_5 + i\Phi_6 \end{aligned} \tag{4.1}$$

Any quantum field theory is determined by the Lagrangian of the theory. A simple Lagrangian will be considered and will show the key results needed for this thesis. The Path Integral Method shall be used for the following calculation. This method is seen in detail in [57].

Consider the following Lagrangian

$$\mathcal{L} = \frac{1}{2} \text{Tr}(\partial_\mu X \partial^\mu X) - \frac{m^2}{2} \text{Tr}(X^2)$$

where X is a matrix X_{ij} where $i, j=1, 2, \dots, N$ and $X=X^\dagger$. The source term, which is included so as to calculate the propagator, is given by $\text{Tr}(JX)$ where J is a Hermitian matrix and the trace is cyclic. The inclusion of this source term results in the following Lagrangian

$$\mathcal{L} = \frac{1}{2} \partial_\mu X_{ij} \partial^\mu X_{ji} - \frac{m^2}{2} X_{ij} X_{ji} + J_{ij} X_{ji} \quad (4.2)$$

As a source as been included to the system, the matrix field must be shifted to ensure that the peak of the Gaussian sits at the origin. The shift is

$$X_{ij} = X'_{ij} + X_{ij_{max}} \quad (4.3)$$

where X'_{ij} is the new field and $X_{ij_{max}}$ is the value of X_{ij} at the maximum of the Gaussian. Using this shift the Lagrangian becomes

$$\mathcal{L} = \frac{1}{2} \partial_\mu X'_{ij} \partial^\mu X'_{ij} - \frac{m^2}{2} X'_{ij} X'_{ji} + \frac{1}{2} J_{ij} X_{ji_{max}} \quad (4.4)$$

In order to calculate correlators for this system, the generating functional must be considered

$$Z[J] = \int [DX'] e^{\int d^4x (\frac{i}{2} \partial_\mu X'_{ij} \partial^\mu X'_{ji} - i \frac{m^2}{2} X'_{ij} X'_{ji} + \frac{i}{2} J_{ij} X_{ji_{max}})} \quad (4.5)$$

which can be rewritten as

$$\begin{aligned} Z[J] &= e^{\int d^4x \frac{i}{2} J_{ij} X_{ji_{max}}} \int [DX'] e^{\int d^4x (\frac{i}{2} \partial_\mu X'_{ij} \partial^\mu X'_{ji} - i \frac{m^2}{2} X'_{ij} X'_{ji})} \\ &= e^{\int d^4x \frac{i}{2} J_{ij} X_{ji_{max}}} \int [DX'] e^{iS'} \end{aligned} \quad (4.6)$$

where

$$S' = \int d^4x (\frac{1}{2} \partial_\mu X'_{ij} \partial^\mu X'_{ij} - \frac{m^2}{2} X'_{ij} X'_{ji}) \quad (4.7)$$

For the system considered to be correctly normalized,

$$\int [DX] e^{iS} = 1$$

resulting in

$$Z[J] = e^{\int d^4x \frac{i}{2} J_{ij} X_{ijmax}} \quad (4.8)$$

Correlation functions are thus generated by computing

$$\frac{1}{i^n} \frac{\delta^n Z}{\delta J_{ij}(x_1) \dots \delta J_{kl}(x_n)} \Big|_{J=0} = \int [DX] X_{ij}(x_1) \dots X_{kl}(x_n) e^{iS}$$

But before any correlation function can be computed, X_{ijmax} must be computed. By computing the maximum of the action obtained from equation (4.2)

$$(\partial_\mu \partial^\mu + m^2) X_{ijmax} = J_{ij}$$

Using Green's function, the following is obtained

$$X_{ijmax} = i \int d^4y \Delta_F(x-y) J_{ij}(y) \quad (4.9)$$

or

$$\Delta_F(x-y) = \int \frac{d^4k}{(2\pi)^4} \frac{i e^{ik(x-y)}}{k^2 - m^2}$$

Thus equation (4.8) becomes

$$Z[J] = e^{\frac{i}{2} \int d^4x J_{ij} i \int d^4y \Delta_F(x-y) J_{ij}(y)} \quad (4.10)$$

Calculating the two point function gives

$$\begin{aligned} \langle X_{ab}(x) X_{cd}(y) \rangle &= - \frac{\delta^2 Z[J]}{\delta J_{ab}(x) \delta J_{cd}(y)} \Big|_{J=0} \\ &= \delta_{ad} \delta_{cb} \Delta_F(x-y) \\ &= \delta_{ad} \delta_{cb} \int \frac{d^4k}{(2\pi)^4} \frac{i e^{ik(x-y)}}{k^2 - m^2} \end{aligned} \quad (4.11)$$

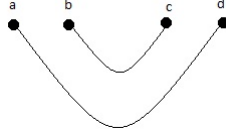


Figure 4.1: The propagator for $\langle X_{ab}(x)X_{cd}(y) \rangle$

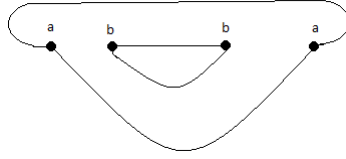


Figure 4.2: The propagator for $\langle X_{ab}(x)X_{ba}(x) \rangle$

Using the two point function, the Feynman diagram for the propagator can be obtained. From (4.11), it can be seen that the propagator is

$$\delta_{ad}\delta_{cb}\Delta_F(x-y)$$

This would correspond to the Feynman diagram as seen in figure 4.1. In what follows, the spacetime dependence is suppressed as it can be trivially determined by conformal invariance.

Now consider the following correlator

$$\langle Tr(X^2) \rangle = \langle X_{ab}X_{ba} \rangle \quad (4.12)$$

The result for this is

$$\delta_{aa}\delta_{bb} = N^2 \quad (4.13)$$

The corresponding diagram to this can be seen in figure 4.2.

Each loop in figure 4.2 is equal to N , as there are two loops, the propagator is N^2 , in agreement with (4.13).

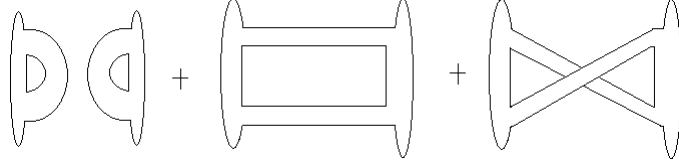


Figure 4.3: $\langle Tr(X^2)Tr(X^2) \rangle$

These ribbon diagrams can be drawn for any trace correlator, with each loop corresponding to an N (when an $N \times N$ matrix field theory is considered). Using these ribbon diagrams, two important results can be seen. The first result shows why large N is a classical limit and the second result shows the breakdown of the planar approximation.

To see that large N is a classical limit, consider the following example:

$$\begin{aligned} \langle Tr(X^2)Tr(X^2) \rangle &= N^4 + 2N^2 \\ &= N^4 \left(1 + \frac{2}{N^2} \right) \end{aligned} \quad (4.14)$$

This corresponds to the ribbon diagrams of figure (4.3).

Taking $N \rightarrow \infty$

$$\begin{aligned} \langle tr(X^2)tr(X^2) \rangle &\approx N^4 \\ &= N^2 N^2 \\ &= \langle tr(X^2) \rangle \langle tr(X^2) \rangle \end{aligned}$$

In general, we have (at large N)

$$\begin{aligned} \langle O_1 O_2 O_3 \dots O_n \rangle &= \langle O_1 \rangle \langle O_2 \rangle \dots \langle O_n \rangle \\ &= \sum_{i_1} \mu_{i_1} O_1(i_1) \sum_{i_2} \mu_{i_2} O_2(i_2) \dots \sum_{i_n} \mu_{i_n} O_n(i_n) \end{aligned}$$

where O is any gauge invariant operator and μ_i is the probability of finding operator i in state i . This is true for all n . This implies that $\mu_i = 1$, $\mu_j = 0$

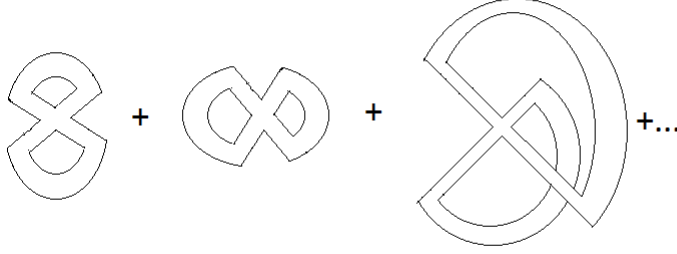


Figure 4.4: $\langle Tr(X^4) \rangle$

when $j \neq i$ for some state i . This means that there is only one solution and it is the “classical” solution. This classical solution was obtained by considering the large N limit only.

The next important result which can be seen from these ribbon diagrams is the breakdown of the planar approximation. Consider

$$\langle Tr(X^4) \rangle = 2N^3 + N$$

The ribbon diagram associated with this can be seen in figure 4.4. The first two ribbon diagrams in figure 4.4 are the planar diagrams, the third ribbon diagram in figure 4.4 is a non-planar diagram as it is a torus shape. More ribbon diagrams can be drawn as the number of matrices considered increases. In general

$$\begin{aligned} \langle tr(X^n) \rangle &= c_0 N^{\frac{n}{2}+1} + c_1 N^{\frac{n}{2}-1} + \dots \\ &= c_1 \left[\frac{c_0}{c_1} N^{\frac{n}{2}+1} + N^{\frac{n}{2}-1} + \dots \right] \end{aligned}$$

where c_0 are the number of planar diagrams for correlation function, c_1 are the number of torus contributions for the correlation function, n is the number

of operators and

$$\frac{c_0}{c_1} \sim n^{-4}$$

Substituting this in gives

$$\langle \text{tr}(X^n) \rangle = c_1 [n^{-4} N^{\frac{n}{2}+1} + N^{\frac{n}{2}-1} + ..$$

When $n \sim \sqrt{N}$ then

$$\langle \text{tr}(X^n) \rangle = c_1 [N^{\frac{n}{2}-1} + N^{\frac{n}{2}-1} + ...] \quad (4.15)$$

From equation (4.15), it can be seen that the torus contribution is the same size as the non-planar contribution. This is the breakdown of the planar limit. As more non-planar diagrams are summed up, their contribution can overpower the planar contribution. It is not possible to sum just the planar diagrams unless $n \ll \sqrt{N}$. For this reason restricted Schur Polynomials, as discussed in the next section, are used as a basis as they allow one to take into consideration all possible contributions (planar and non-planar).

4.2 Schur Polynomials

Schur polynomials are useful tools in describing giant gravitons on the quantum field side of the AdS/CFT correspondence. This is because Schur Polynomials are a complete set of gauge invariant field operators in the quantum field theory and the free field two point correlator of Schur Polynomials is simple. Schur Polynomials are characters of the unitary group in their irreducible representations where the irreducible representations R are labelled using Young diagrams. Schur Polynomials are classified into two main types: unrestricted and restricted. It must be noted that the tools for calculating Schur Polynomials have been developed over many years. In this chapter,

the results of previous research will be shown. Full derivations of the results shown in this chapter can be seen in [3, 4, 6, 8].

4.2.1 Schur Polynomials- Unrestricted

An unrestricted Schur Polynomial is defined as follows

$$\chi_R(Z) = \frac{1}{n!} \sum_{\sigma \in S_n} \chi_R(\sigma) Z_{i\sigma(1)}^{i_1} \dots Z_{i\sigma(n)}^{i_n} \quad (4.16)$$

where $\chi_R(\sigma)$ is a character of an element σ of the symmetric group S_n in the irreducible representation R . In general the character is defined as follows

$$\chi_R(\sigma) = tr(\Gamma_R(\sigma))$$

where R is a representation of S_n . R is labelled by a Young Diagram with n boxes as there is a one-to-one correspondence between an irreducible representation of the symmetric group S_n and Young Diagrams. Young Diagrams also label $SU(N)$ tensors. A Young Diagram comprised of n boxes in a single column corresponds to a completely antisymmetric tensor with n indices. A Young Diagram comprised of m boxes in a single row corresponds to a completely symmetric tensor with m indices [15]. Z^1 is a complex scalar field. The lower index on the Z is permuted as specified by σ . The product of the Z s above for a given σ will give a product of traces of Z s. (Note: $Z^i_i = tr(Z)$)

Some properties of these Schur Polynomials can be seen in equations (4.17), (4.18), (4.19).

$$\langle \chi_R \chi_R^\dagger \rangle = f_R \quad (4.17)$$

¹In section 4.1, the symbol X was used to denote the complex scalar field so as not to confuse the complex scalar field Z with the generating functional $Z[J]$. For the rest of this thesis, the symbol X will be replaced by Z .

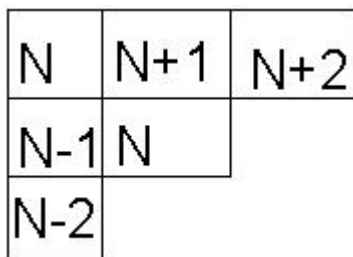


Figure 4.5: A Young Diagram with the weight of each block displayed

$$\langle \chi_R(Z) \chi_S^\dagger(Z) \rangle = f_R \delta_{RS} \quad (4.18)$$

$$\chi_R \chi_S = f_{RST} \chi_T \quad (4.19)$$

In equation (4.17) and (4.18), f_R is the product of the weights of the boxes comprising the Young Diagram. The weights of the Young Diagram increase by one as one moves across (left to right) the Young Diagrams and decrease by one as one moves down the Young Diagrams. An example of a Young Diagram with the weights filled in can be seen in figure 4.5.

Equation (4.18) is the exact two point correlation function of the Schur Polynomials. From the presence of the delta function, it can be seen that the correlator is diagonal in representations, that is, all non-diagonal elements are zero. Correlation functions are the basic observables of any quantum field theory so it is extremely useful to have such explicit formulas. From the section on matrix models, it was seen that the number of loops obtained from taking traces of the matrices will give N to some power. In equation (4.19), the product of two Schur Polynomials is shown to be the sum of many different Schur Polynomials with coefficients the Littlewood Richardson numbers. This product rule is known as the Littlewood- Richardson rule. If represen-

tation R is a Young Diagram with n boxes and representation S is a Young Diagram with m boxes then representation T is a Young Diagram with $n+m$ boxes. f_{RST} are the Littlewood Richardson numbers. This product rule is useful as it can be used to break up any product of Schur Polynomials in to a sum of Schur Polynomials [15].

The two point function of these Schur Polynomials can be calculated exactly with the result (4.17) [1]. The two point correlation function as seen in equation (4.18) can be rewritten as

$$\langle \chi_R(Z)\chi_S(Z^*) \rangle = \delta_{RS} \frac{D_R n_R!}{d_R} \quad (4.20)$$

where D_R is the dimension of the representation R of the unitary group and d_R is the dimension of the representation R of the permutation group. The dimension of the representation R of the unitary group D_R is given by

$$D_R = \frac{f_R}{hooks_R}$$

and the dimension of the representation R of the permutation group is given by

$$d_r = \frac{n!}{hooks_R}$$

In these equations, f_R is again the product of the weights of the boxes and the hook lengths of the representation R are given by summing the number of boxes below the box and the number of boxes to the right of the block plus the block itself. An example of a Young Diagram with the hook lengths filled in can be seen in figure 4.6.

It is further possible to consider the two point correlation function with some spacetime dependence x,y . In this case the two point correlation func-

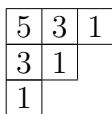


Figure 4.6: A Young Diagram with the hook length displayed in each box

tion is [1]

$$\langle \chi_R(Z(x))\chi_S(Z^*(y)) \rangle = \delta_{RS} \frac{D_R n_R!}{d_R} \frac{1}{(x-y)^{2n_R}} \quad (4.21)$$

In the work presented in this thesis, Schur Polynomials without a space-time dependence are considered. As mentioned earlier, the spacetime dependence plays a trivial role since it is completely determined by conformal invariance.

How to remove a box

It is possible to obtain an expression for the case where one block is removed from the Young Diagram. This is known as the reduction rule. In general for unrestricted Schur Polynomials

$$\frac{d}{dZ_i} \chi_R(Z) = \sum_{R'} C_{RR'} \chi_{R'}(Z) \quad (4.22)$$

In this equation, R' is a representation obtained when one block is removed from the Young Diagram. As there may be many different possible ways to remove a block from the particular representation, each possible resulting representation must be considered. Thus there is a summation over R' . $C_{RR'}$ is the weight of the block pulled off the Young Diagram. $\chi_{R'}(Z)$ is the Schur Polynomial associated with the representation R' . From the representation theory of the symmetric group it is known that R (an irreducible representation of S_n) subduces all possible R' when restricted to an S_{n-1} subgroup:

$$\Gamma_R = \begin{bmatrix} \Gamma_{R'_1} & 0 & \dots \\ 0 & \Gamma_{R'_2} & \dots \\ \dots & \dots & \dots \\ 0 & 0 & \Gamma_{R'_i} \end{bmatrix} \quad (4.23)$$

In equation (4.23), the number of R' subspaces i depends on the irreducible representation of S_n being considered. In general, the number of irreducible representations of a group is equal to the number of conjugacy classes within the group R . An example of the reduction of an unrestricted Schur Polynomial is as follows

$$\frac{d}{dZ_i} \chi_{\begin{smallmatrix} \square \\ \square \end{smallmatrix}}(Z) = (N+1)\chi_{\begin{smallmatrix} \square \\ \square \end{smallmatrix}}(Z) + (N-1)\chi_{\begin{smallmatrix} \square \\ \square \end{smallmatrix}}(Z) \quad (4.24)$$

It was suggested in [1] that the completely antisymmetric representation (for example $\begin{smallmatrix} \square \\ \square \end{smallmatrix}$) with $\mathcal{O}(N)$ boxes in the column is dual to a sphere giant whereas the completely symmetric representation (for example $\begin{smallmatrix} \square \\ \square \end{smallmatrix}$) is dual with $\mathcal{O}(N)$ boxes in the row to an AdS giant.

4.2.2 Schur Polynomials- Restricted

Excitation of giant gravitons are obtained by attaching open strings to giant gravitons. The dual to this in the conformal field theory is the restricted Schur Polynomial [3, 4, 6]

$$\chi_{R,R_\alpha}(Z, Y) = \frac{1}{n!m!} \sum_{\sigma \in S_{n+m}} Tr_{R_\alpha}(\Gamma_R(\sigma)) Tr(\sigma Z^{\otimes n} \otimes Y^{\otimes m}) \quad (4.25)$$

where

$$Tr(\sigma Z^{\otimes n} \otimes Y^{\otimes m}) = Z_{i\sigma(1)}^{i_1} \dots Z_{i\sigma(n)}^{i_n} Y_{i\sigma(n+1)}^{i_{n+1}} \dots Y_{i\sigma(n+m)}^{i_{n+m}}$$

In this expression, R is an irreducible representation of S_{n+m} and is labelled by the Young Diagram with $n+m$ boxes. R_α is an irreducible representation

of $S_n \times S_m$ and is labelled by two Young Diagrams, one with n boxes, the other with m boxes. The R_α is interchangeable with the label (r,s) . $S_n \times S_m$ is a subgroup of S_{n+m} in which S_n acts on n indices of the Z 's and S_m acts on m indices of the Y 's. The trace $\text{Tr}_{R_\alpha}(\Gamma_R(\sigma))$ is a restricted trace of the group elements of $\sigma \in S_{n+m}$ in the irreducible representation R . By restricting R to the $S_n \times S_m$ subgroup, R will in general be reducible. The irreducible representations subduced are labelled R_α . The restricted trace corresponds to taking the trace over the R_α subspace [8].

As in the previous section, the exact two point correlation function for the restricted Schur Polynomials can be obtained [8]

$$\langle \chi_{R,(r_{\alpha 1}, r_{\alpha 2})} \chi_{S,(s_{\beta 1}, s_{\beta 2})}^\dagger \rangle = \delta_{RS} \delta_{(r_{\alpha 1} s_{\beta 1})} \delta_{(r_{\alpha 1} s_{\beta 2})} \frac{(hooks)_R}{(hooks)_{r_{\alpha 1}} (hooks)_{r_{\alpha 2}}} f_R \quad (4.26)$$

where f_R is the product of the weights of the boxes comprising the Young Diagram and the hook length of a box is calculated as seen previously.

How to remove a box

As with the case for the unrestricted Schur Polynomial, in order to study the action of the Dilatation Operator on the restricted Schur Polynomial, a reduction rule must be obtained. However, the reduction rule for the restricted Schur Polynomial is not as straight forward as the unrestricted case. In some cases, calculating the reduction of a restricted Schur Polynomial means having to calculate projection operators. An example of the reduction of a restricted Schur Polynomial where the calculation of projection operators is not needed can be seen as follows

$$\frac{d}{dY_j^j} \chi_{R,R'}(Z, Y) = \frac{d}{dY_j^j} \frac{1}{n!1!} \sum_{\sigma \in S_{n+1}} \text{Tr}_{R'}(\Gamma_R(\sigma)) Z_{i\sigma(1)}^{i_1} \dots Z_{i\sigma(n)}^{i_n} Y_{i\sigma(n+1)}^{i_{n+1}}$$

where R' is an irreducible representation of S_n . By explicit computations, one gets the following result

$$\frac{d}{dY_j^j} \chi_{R,R'}(Z, Y) = C_{R,R'} \chi_{R'}(Z) \quad (4.27)$$

where $C_{R,R'}$ is the weight of the Y block removed from the Young Diagram.

Another example of this easy removal of a block can be seen when one considers the representation composed of n Z's, one Y and one W

$$\frac{d}{dW_j^j} \chi_{R,R''}(Z, Y, W) = \frac{d}{dW_j^j} \frac{1}{n!} \sum_{\sigma \in S_{n+2}} Tr_{R''}(\Gamma_R(\sigma)) Z_{i\sigma(1)}^{i_1} \dots Z_{i\sigma(n)}^{i_n} Y_{i\sigma(n+1)}^{i_{n+1}} W_{i\sigma(n+2)}^{i_{n+2}}$$

where R is an irreducible representation of S_{n+2} , R' is an irreducible representation of S_{n+1} (one box removed) and R'' is an irreducible representation of S_n (two boxes removed). For this sort of example, the chain of subgroups must be specified. The S_{n+1} subgroup leaves $n+2$ inert. The S_n subgroup leaves $n+2$ and $n+1$ inert. R'' is subduced from R' which is an irreducible representation of S_{n+1} . Again, explicit computation shows

$$\frac{d}{dW_j^j} \chi_{R,R''}(Z, Y, W) = C_{R,R'} \chi_{R',R''}(Z, Y) \quad (4.28)$$

where $C_{R,R'}$ is the weight of the W block removed from the Young Diagram R to obtain R' .

Again, this is a relatively easy calculation as the action of the “derivative” acts on the $\{n+2\}$ element of the group thus resulting in an expression in terms of the S_{n+1} subgroup whose elements are $\sigma \in S_{n+1} = \{1, 2, \dots, n+1\}$. See [3] for further details. However, if one were to consider the following

$$\frac{d}{dY_j^j} \chi_{R,R'}(Z, Y, W) = \frac{d}{dY_j^j} \frac{1}{n!} \sum_{n \in S_{n+2}} Tr_{R'}(\Gamma_R(\sigma)) Z_{i\sigma(1)}^{i_1} \dots Z_{i\sigma(n)}^{i_n} Y_{i\sigma(n+1)}^{i_{n+1}} W_{i\sigma(n+2)}^{i_{n+2}}$$

then the “derivative” would act on the $n+1$ term. In this case, the projection operator needs to be rewritten in terms of the projector defined by a different

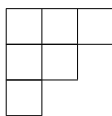


Figure 4.7: Representation R

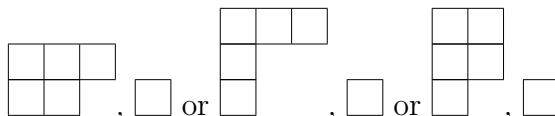


Figure 4.8: R'_1, R'_2, R'_3 respectively

chain of subgroups. The projection operator is defined by stating what space it acts in and what subspace it projects to. This can be done by specifying a Young Diagram (what space it acts in) and specifying boxes to be removed and the order in which they must be removed (what subspace it projects to). Consider the irreducible representation R of figure 4.7.

R can be decomposed into three possible subspaces when one box is removed. These possible subspaces are shown in figure 4.8.

The subspace into which one projects must be stated explicitly. The projection operator constructed for this will not only then project into the correct subspace but will also ensure that the other possible subspaces give a zero contribution. It was seen in (4.23) that the trace of the representation R is like that of the sum of the traces of the individual subspaces.

Suppose the subspace $\begin{array}{|c|c|} \hline \square & \square \\ \hline \square & \square \\ \hline \end{array}$ is chosen as the subspace into which one projects, then the projection operator will be chosen in such a way that the contributions from $\begin{array}{|c|c|c|} \hline \square & \square & \square \\ \hline \square & \square & \square \\ \hline \square & \square & \square \\ \hline \end{array}$ and $\begin{array}{|c|c|} \hline \square & \square \\ \hline \square & \square \\ \hline \square & \square \\ \hline \end{array}$ are zero.

Generally, what is studied is the case where two or more boxes are removed. Where two boxes are removed, the correct projectors again need to

be considered. The possible projectors can be seen by removing another box from the R' subspaces. In this example, where $\sigma \in S_4$, there are two places where a box can be removed from each R' . The spaces subduced from R'_i are labelled R''_j .

$$\Gamma_{\begin{array}{|c|c|c|} \hline \square & \square & \square \\ \hline \square & & \\ \hline \square & & \\ \hline \end{array}} = \begin{bmatrix} \Gamma_{\begin{array}{|c|c|} \hline \square & \square \\ \hline \square & \\ \hline \end{array}} & 0 & 0 & 0 & 0 & 0 \\ 0 & \Gamma_{\begin{array}{|c|c|c|} \hline \square & \square & \square \\ \hline \square & & \\ \hline \end{array}} & 0 & 0 & 0 & 0 \\ 0 & 0 & \Gamma_{\begin{array}{|c|c|} \hline \square & \square \\ \hline \square & \\ \hline \end{array}} & 0 & 0 & 0 \\ 0 & 0 & 0 & \Gamma_{\begin{array}{|c|c|c|} \hline \square & \square & \square \\ \hline \square & & \\ \hline \end{array}} & 0 & 0 \\ 0 & 0 & 0 & 0 & \Gamma_{\begin{array}{|c|c|} \hline \square & \square \\ \hline \square & \\ \hline \end{array}} & 0 \\ 0 & 0 & 0 & 0 & 0 & \Gamma_{\begin{array}{|c|c|} \hline \square & \square \\ \hline \square & \\ \hline \end{array}} \end{bmatrix} \quad (4.29)$$

Again, the subspace desired must be explicitly stated in order to use the correct projector. Notice in (4.29) that the same Young Diagrams appear along the diagonal of the matrix. It must be noted that the $\Gamma_{R_{11}}$ entry does not equal that of the $\Gamma_{R_{55}}$ entry even though they have the same Young Diagram. This is because the $\Gamma_{R_{11}}$ entry came from reducing the R'_1 subspace whereas the $\Gamma_{R_{55}}$ entry came from reducing the R'_3 subspace. Clearly, the order in which boxes are removed from R is important. It can also be noted that all the combinations with which a box can be removed, must be considered, with the necessary projector built in order that only the wanted subgroup remains.

From the definition of the restricted Schur Polynomial, it can be seen that the restricted character $\text{Tr}_{R_\alpha} (\Gamma_R(\sigma))$ must also be calculated. However, not much is known about the restricted character. The restricted Schur Polynomial needs to be rewritten in terms of a basis which can be easily manipulated. This is easily done by considering the original representation

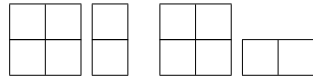
R with the blocks that are to be removed labelled on the Young Diagram rather than the considering the representations R' that one projects to. This is the Young-Yamouuchi basis. For example rather than considering

$$\chi_{\begin{array}{|c|c|c|} \hline \square & \square & \square \\ \hline \square & & \\ \hline \square & & \end{array}; \begin{array}{|c|c|} \hline \square & \square \\ \hline \square & \square \\ \hline \square & \square \\ \hline \end{array}}(Z, Y) = \frac{1}{4!2!} \sum_{n \in S_6} Tr_{\begin{array}{|c|c|} \hline \square & \square \\ \hline \square & \square \\ \hline \end{array}}(\Gamma_{\begin{array}{|c|c|c|} \hline \square & \square & \square \\ \hline \square & & \\ \hline \square & & \end{array}}(\sigma)) Tr(\sigma) Z_{i\sigma(1)}^{i_1} \dots Z_{i\sigma(4)}^{i_4} Y_{i\sigma(5)}^{i_5} Y_{i\sigma(6)}^{i_6} \quad (4.30)$$

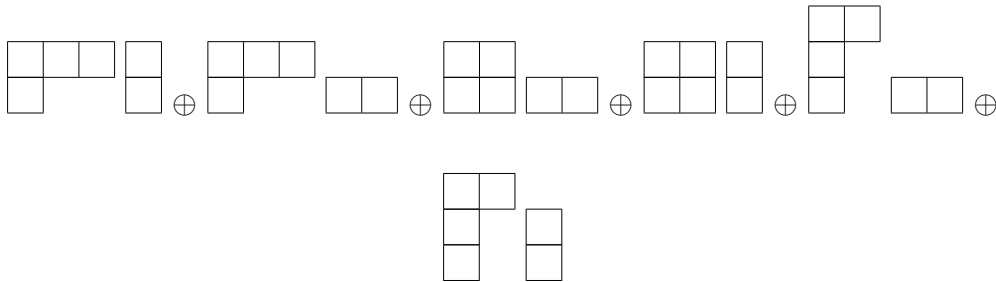
it is easier to consider

$$\chi_{\begin{array}{|c|c|c|} \hline \square & \square & * \\ \hline \square & & \\ \hline * & & \end{array}}(Z, Y) = \frac{1}{4!} \sum_{n \in S_6} Tr_{\begin{array}{|c|c|} \hline \square & * \\ \hline \square & \\ \hline * & \end{array}}(\Gamma_{\begin{array}{|c|c|c|} \hline \square & \square & \square \\ \hline \square & & \\ \hline \square & & \end{array}}(\sigma)) Tr(\sigma) Z_{i\sigma(1)}^{i_1} \dots Z_{i\sigma(4)}^{i_4} Y_{i\sigma(5)}^{i_5} Y_{i\sigma(6)}^{i_6} \quad (4.31)$$

where the blocks containing * are the blocks which are removed. There are two different ways of arranging the blocks removed



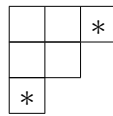
By summing over all possible ways to remove boxes, the following $S_4 \times S_2$ irreducible representations can be subduced from R



One way to check that all the subduced representations have been caught is by summing the dimensions of all the subduced representations and comparing with the dimension of representation R. The dimensions are calculated

using the method as shown previously. The dimensions of the representations obtained are 3, 3, 2, 2, 3 and 3 respectively. The sum of this is 16 which is the exact dimension of R so all possible subduced representations have been obtained.

It is necessary to only construct the operator which assembles the removed boxes in the correct way to produce s. Using the example as seen already



The corresponding projector will act in the subspace spanned by two sets of states

$$|1\rangle = \left| \begin{array}{|c|c|c|} \hline & & 1 \\ \hline & & \\ \hline 2 & & \\ \hline \end{array} \right\rangle \quad > \quad |2\rangle = \left| \begin{array}{|c|c|c|} \hline & & 2 \\ \hline & & \\ \hline 1 & & \\ \hline \end{array} \right\rangle$$

Using the Young- Yamonouchi basis, each state above could be one of any $d_{\begin{array}{|c|c|} \hline & \\ \hline & \\ \hline \end{array}}=2$ states corresponding to the number of different ways to complete the labels. Now, all that is needed is to supply a formula for the action of $\Gamma_R(\sigma)$ for $\sigma=1,(12)$ when acting on the subspaces $|1\rangle$ and $|2\rangle$. This is done by making the following observation

$$\left| \begin{array}{|c|c|c|} \hline & & \\ \hline & & \\ \hline & & \\ \hline \end{array}, \begin{array}{|c|c|} \hline & \\ \hline & \\ \hline \end{array}, \begin{array}{|c|c|} \hline & \\ \hline & \\ \hline \end{array} \right\rangle = \alpha |1\rangle + \beta |2\rangle$$

where α and β are normalized. For the action of $\Gamma_R((12))$ it is known that

$$\Gamma_R((12)) \left| \begin{array}{|c|c|c|} \hline & & \\ \hline & & \\ \hline & & \\ \hline \end{array}, \begin{array}{|c|c|} \hline & \\ \hline & \\ \hline \end{array}, \begin{array}{|c|c|} \hline & \\ \hline & \\ \hline \end{array} \right\rangle = \left| \begin{array}{|c|c|c|} \hline & & \\ \hline & & \\ \hline & & \\ \hline \end{array}, \begin{array}{|c|c|} \hline & \\ \hline & \\ \hline \end{array}, \begin{array}{|c|c|} \hline & \\ \hline & \\ \hline \end{array} \right\rangle$$

This action of $\Gamma_R(\sigma)$ on any Young-Yamonouchi state is well known and can be calculated using strand diagrams. Strand diagrams are invented in

Appendix B3 of [6]. Using strand diagrams, the values for α and β can be obtained

$$\left| \begin{array}{c} \square\square\square \\ \square\square \\ \square \end{array}, \begin{array}{c} \square\square \\ \square \end{array}, \begin{array}{c} \square\square \end{array} \right\rangle = \sqrt{\frac{5}{8}} |1\rangle + \sqrt{\frac{3}{8}} |2\rangle$$

This result can be substituted back into (4.15) to obtain

$$\chi_{\begin{array}{c} \square\square\square \\ \square\square \\ \square \end{array}; \begin{array}{c} \square\square \\ \square \end{array}, \begin{array}{c} \square\square \end{array}}(Z, Y) = \frac{5}{16} \chi_{\begin{array}{c} \square\square\square \\ \square\square \\ \square \\ \square \end{array}} \begin{array}{c} 1 \\ \square \end{array} (Z, Y) + \frac{3}{16} \chi_{\begin{array}{c} \square\square\square \\ \square\square \\ \square \\ \square \end{array}} \begin{array}{c} 2 \\ \square \\ 1 \end{array} (Z, Y) \quad (4.32)$$

Using the projection operator, the restricted trace can be rewritten as follows

$$Tr_{R_\alpha}(\Gamma_R(\sigma)) = Tr_R(P_{R \rightarrow R_\alpha} \Gamma_R(\sigma)) \quad (4.33)$$

It is difficult to write down an explicit formula for the projection operator as it is possible that the representation (r,s) can be subduced more than once when irreducible representation R is decomposed into the irreducible representations of the $S_n \times S_m$ subgroup. When studying an irreducible representation R whose Young Diagram has at most two columns this problem does not arise and then it is possible to write down a general expression for the projection operator. For more than two columns, the multiplicity of the problem is non trivial to solve. For the case where there are at most two columns in the Young Diagram considered the projection operator is

$$P_s = \frac{d_s}{m!} \sum_{\sigma \in S_m} \chi_s(\sigma) \Gamma_R(\sigma) \quad (4.34)$$

How to grow a box

When considering the Dilatation Operator, it can be seen that not only does one remove boxes from the Young Diagram considered but one also “grows” the boxes back on[4].

Consider

$$\chi_{R,R'}(Z, Y) = \frac{1}{n!} \sum_{\sigma \in S_{n+1}} Tr_{R'}(\Gamma_R(\sigma)) Z_{i\sigma(1)}^{i_1} \dots Z_{i\sigma(n)}^{i_n} Y_{i\sigma(n+1)}^{i_{n+1}} \quad (4.35)$$

In equation (4.20), R is an irreducible representation of S_{n+1} and R' is an irreducible representation of S_n . In order to obtain the expression for “growing” a box, it is necessary to rewrite the sum over S_{n+1} as a sum over the cosets of an S_n subgroup which leaves $n+1$ unchanged ($\sigma(n+1) = n+1$). After rearranging one will get

$$\begin{aligned} \chi_{R,R'}(Z, Y) - \chi_{R'}(Z) Tr(Y) &= \frac{1}{n!} \sum_{\sigma \in S_n} \left[Tr_{R'}(\Gamma_R[\sigma(1, n+1)])(ZY)_{i\sigma(1)}^{i_1} (Z)_{i\sigma(2)}^{i_2} \dots Z_{i\sigma(n)}^{i_n} \right. \\ &\quad + Tr_{R'}(\Gamma_R[\sigma(2, n+1)])(Z)_{i\sigma(1)}^{i_1} (ZY)_{i\sigma(2)}^{i_2} \dots Z_{i\sigma(n)}^{i_n} + \dots + \\ &\quad \left. + Tr_{R'}(\Gamma_R[\sigma(n, n+1)])(Z)_{i\sigma(1)}^{i_1} (Z)_{i\sigma(2)}^{i_2} \dots (ZY)_{i\sigma(n)}^{i_n} \right] \end{aligned} \quad (4.36)$$

where $\chi_{R'}(Z)$ is a Schur Polynomial. Introduce the notation $Y^+ = (ZY)$ and focus on the first term in (4.36). This term can be rewritten as a sum over the S_{n-1} subgroup of S_n which comprises of all permutations which leave 1 fixed

$$\begin{aligned} &\frac{1}{n!} \sum_{\sigma \in S_n} Tr_{R'}(\Gamma_R[\sigma(n+1, 1)])(Y^+)_{i\sigma(1)}^{i_1} (Z)_{i\sigma(2)}^{i_2} \dots Z_{i\sigma(n)}^{i_n} \\ &= \frac{1}{n!} \sum_{\sigma \in S_{n-1}} Tr_{R'}(\Gamma_R[\sigma(n+1, 1)]) Tr(Y^+) (Z)_{i\sigma(2)}^{i_2} \dots Z_{i\sigma(n)}^{i_n} \\ &\quad + \frac{1}{n!} \sum_{\sigma \in S_{n-1}} Tr_{R'}(\Gamma_R[\sigma(1, 2)(n+1, 1)])(Y^+ Z)_{i\sigma(2)}^{i_2} \dots Z_{i\sigma(n)}^{i_n} + \dots + \\ &\quad + \frac{1}{n!} \sum_{\sigma \in S_{n-1}} Tr_{R'}(\Gamma_R[\sigma(1, n)(n+1, 1)])(Z)_{i\sigma(2)}^{i_2} \dots (Y^+ Z)_{i\sigma(n)}^{i_n} \end{aligned}$$

R' can be broken up into $R' = \oplus_{\alpha} R''_{\alpha}$ where the sum runs over all representations R''_{α} that can be obtained from R' by removing a box. The subgroup

that is summed leaves both 1 and (n+1) unchanged so that

$$\Gamma_R(\tau)\Gamma_R[(n+1, 1)] = \Gamma_R[(n+1, 1)]\Gamma_R(\tau).$$

By Schur's Lemma, this implies that $\Gamma_R[(n+1, 1)]$ is proportional to the identity when acting on the R''_α subspace

$$\langle a, R''_\alpha | \Gamma_R[(n+1, 1)] | b, R''_\alpha \rangle = \lambda_\alpha \delta_{ab}$$

By decomposing the trace over R' , one can write

$$Tr_{R'}(\Gamma_R[\tau(1, n)(n+1, 1)]) = \sum_{\alpha} Tr_{R''_\alpha}(\Gamma_R[\tau(1, n)(n+1, 1)])$$

Making use of projectors and the block structure of $\Gamma_R[\tau]$ as already seen in this chapter, the following is obtained [4]

$$Tr_{R'}(\Gamma_R[\tau(1, i)(i+1, 1)]) = \sum_{\alpha} \lambda_\alpha Tr_{R''_\alpha}(\Gamma_R[\tau(1, i)])$$

where i is fixed. Thus

$$\begin{aligned} & \frac{1}{n!} \sum_{\sigma \in S_n} Tr_{R'}(\Gamma_R[\sigma(n+1, 1)])(Y^+)_{i\sigma(1)}^{i_1} (Z)_{i\sigma(2)}^{i_2} \dots Z_{i\sigma(n)}^{i_n} \\ &= \frac{1}{n!} \sum_{\alpha} \lambda_\alpha \sum_{\sigma \in S_n} Tr_{R''_\alpha}(\Gamma_{R'}[\sigma])(Y^+)_{i\sigma(1)}^{i_1} (Z)_{i\sigma(2)}^{i_2} \dots Z_{i\sigma(n)}^{i_n} \\ &= \frac{1}{n} \sum_{\alpha} \lambda_\alpha \chi_{R', R''_\alpha}^{(1)}(Z, Y^+) \end{aligned}$$

It can be seen that the n terms on the right hand side of (4.36) make the same contribution to give

$$\chi_{R, R'}^{(1)}(Z, Y) - \chi_{R'}(Z)Tr(Y) = \sum_{\alpha} \lambda_\alpha \chi_{R', R''_\alpha}^{(1)}(Z, Y^+)$$

where it was found in [3] that

$$\lambda_\alpha = \frac{1}{c_{RR'} - c_{R'R''_\alpha}} \quad (4.37)$$

where $c_{RR'}$ is the weight of the box removed from R to obtain R' and $c_{R'R''_\alpha}$ is the weight of the box removed from R' to obtain R'' .

Making this substitution gives

$$\chi_{R,R'}^{(1)}(Z, Y) - \chi_{R'}(Z)Tr(Y) = \sum_{\alpha} \frac{1}{c_{RR'} - c_{R'R''_\alpha}} \chi_{R',R''_\alpha}^{(1)}(Z, Y^+) \quad (4.38)$$

From the results described in this chapter, it is now possible to find the Hamiltonian. To do this the action of the dilatation operator on the restricted Schur Polynomial must be considered. The steps that must be completed to do this are

- act with D on χ
- go to $\chi_{R'R''}$ basis
- reduce
- evaluate characters
- grow a box
- go back to $\chi_{R,(r,s)}$ basis
- Normalization

This is a long and difficult process that involves the inversion of a matrix. It can be seen that a new method for solving this Hamiltonian is needed, starting with the re-evaluation of the action of the one loop dilatation operator on the restricted Schur Polynomial.

Chapter 5

Action of the Dilatation Operator

In this chapter, the action of the one loop dilatation operator on the restricted Schur Polynomial built using two adjoint scalars will be studied. Consider the action of the one loop dilatation operator in the SU(2) sector [45] of the $\mathcal{N} = 4$ super Yang Mills Theory

$$D = -g_{YM}^2 Tr[Y, Z][\partial_Y, \partial_Z]$$

on the restricted Schur Polynomial

$$\chi_{(R,(r,s))}(Z^{\otimes n}, Y^{\otimes m}) = \frac{1}{n!m!} \sum_{\sigma \in S_{n+m}} Tr_{(r,s)}(\Gamma_R(\sigma)) Z_{i\sigma(1)}^{i_1} \cdots Z_{i\sigma(n)}^{i_n} Y_{i\sigma(n+1)}^{i_{n+1}} \cdots Y_{i\sigma(n+m)}^{i_{n+m}}$$

This restricted Schur Polynomial is exactly that which was seen previously in equation (4.25).

Calculating the one loop dilatation operator action on the restricted Schur

Polynomial gives

$$D\chi_{(R,(r,s))}(Z^{\otimes n}, Y^{\otimes m}) = \frac{g_{YM}^2}{(n-1)!(m-1)!} \sum_{\psi \in S_{n+m}} Tr_{(r,s)}(\Gamma_R((n, n+1)\psi - \psi(n, n+1))) \times \\ Z_{i\psi(1)}^{i_1} \dots Z_{i\psi(n-1)}^{i_{n-1}} (YZ - ZY)_{i\psi(n)}^{i_n} \delta_{i\psi(n+1)}^{i_{n+1}} Y_{i\psi(n+2)}^{i_{n+2}} \dots Y_{i\psi(n+m)}^{i_{n+m}} \quad (5.1)$$

The sum ψ runs only over permutations for which $\psi(n+1)=n+1$. In order to perform the sum over the delta function $\delta_{i\psi(n+1)}^{i_{n+1}}$, the sum over S_{n+m} must be written in terms of the sum over the cosets of the S_{n+m-1} subgroup obtained by keeping the permutations that satisfy $\psi(n+1)=n+1$. The result follows from the reduction rule for Schur Polynomials as discussed previously in Chapter 4.

$$D\chi_{(R,(r,s))}(Z^{\otimes n}, Y^{\otimes m}) = \frac{g_{YM}^2}{(n-1)!(m-1)!} \sum_{\psi \in S_{n+m-1}} \sum_{R'} c_{RR'} Tr_{(r,s)}(\Gamma_R((n, n+1))\Gamma_{R'}(\psi) - \\ \Gamma_{R'}(\psi)\Gamma_R((n, n+1))) Z_{i\psi(1)}^{i_1} \dots Z_{i\psi(n-1)}^{i_{n-1}} (YZ - ZY)_{i\psi(n)}^{i_n} Y_{i\psi(n+2)}^{i_{n+2}} \dots Y_{i\psi(n+m)}^{i_{n+m}}$$

The sum over R' runs over all representations that can be subduced from R . In terms of Young Diagrams, R' are all possible Young Diagrams which can be obtained by dropping one box from R . $c_{R,R'}$ is the weight of the box removed from R in order to obtain R' . From Chapter Four, it was seen that for restricted traces one can write

$$\chi_{(R,(r,s))}(\sigma) = Tr_{(r,s)}(\Gamma_R(\sigma)) = Tr(P_{R \rightarrow (r,s)}\Gamma_R(\sigma))$$

This will prove to be useful later on in this calculation. Using the identity and that $\psi(n+1)=n+1$ the following can also be written

$$Z_{i\psi(1)}^{i_1} \dots Z_{i\psi(n-1)}^{i_{n-1}} (YZ - ZY)_{i\psi(n)}^{i_n} Y_{i\psi(n+2)}^{i_{n+2}} \dots Y_{i\psi(n+m)}^{i_{n+m}} = Tr(((n, n+1)\psi - \psi(n, n+1))Z^{\otimes n}Y^{\otimes m})$$

It can be noted that

$$Tr(\sigma Z^{\otimes n}Y^{\otimes m}) = Z_{i\psi(1)}^{i_1} \dots Z_{i\psi(n)}^{i_n} Y_{i\psi(n+1)}^{i_{n+1}} \dots Y_{i\psi(n+m)}^{i_{n+m}}$$

It was proven in [47] that

$$Tr(\sigma Z^{\otimes n} Y^{\otimes m}) = \sum_{T,(t,u)} \frac{d_T n! m!}{d_t d_u (n+m)!} \chi_{T,(t,u)}(\sigma) \chi_{T,(t,u)}(Z, Y)$$

Making these substitutions the following expression is obtained

$$D\chi_{(R,(r,s))}(Z, Y) = g_{YM}^2 \sum_{T,(t,u)} \sum_{\psi \in S_{n+m-1}} \sum_{R'} \frac{c_{RR'} d_T n m}{d_t d_u (n+m)!} Tr_{(r,s)}(\Gamma_R((n, n+1)) \Gamma_{R'}(\psi) - \Gamma_{R'}(\psi) \Gamma_R((n, n+1))) \chi_{T,(t,u)}(\psi(n, n+1) - (n, n+1)\psi) \chi_{T,(t,u)}(Z, Y)$$

By setting

$$M_{R,(r,s);T,(t,u)} = g_{YM}^2 \sum_{\psi \in S_{n+m-1}} \sum_{R'} \frac{c_{RR'} d_T n m}{d_t d_u (n+m)!} Tr_{(r,s)}(\Gamma_R((n, n+1)) \Gamma_{R'}(\psi) - \Gamma_{R'}(\psi) \Gamma_R((n, n+1))) \times \chi_{T,(t,u)}(\psi(n, n+1) - (n, n+1)\psi)$$

then the action of the one loop dilatation operator on the restricted Schur Polynomial can be written as follows

$$D\chi_{(R,(r,s))}(Z, Y) = \sum_{T,(t,u)} M_{R,(r,s);T,(t,u)} \chi_{T,(t,u)}(Z, Y)$$

Using the fundamental orthogonality relation, the sum over ψ can be performed to give

$$M_{R,(r,s);T,(t,u)} = 2g_{YM}^2 \sum_{R'} \frac{c_{RR'} d_T n m}{d_{R'} d_t d_u (n+m)} Tr([\Gamma_R((n, n+1)), P_{R \rightarrow (r,s)}] I_{R'T'} \times [P_{T \rightarrow (t,u)}, \Gamma_T((n, n+1))] I_{T'R}) \quad (5.2)$$

where $I_{R'T'}$ and $I_{T'R}$ are known as the intertwiners. The intertwiners are defined in Appendix B. The action of the one loop dilatation operator on normalized operators must now be considered so as to obtain the spectrum for the anomalous dimensions. It was seen in chapter four that the two point correlation function for the restricted Schur Polynomial is [8]

$$\langle \chi_{R,(r,s)}(Z, Y) \chi_{T,(t,u)}(Z, Y)^\dagger \rangle = \delta_{R,(r,s);T,(t,u)} f_R \frac{hooks_R}{hooks_r hooks_s}$$

As in Chapter four, f_R is the product of the weights in Young Diagram R and $hooks_R$ is the product of the hook lengths in Young Diagram R. The normalized operators can thus be obtained from

$$\chi_{R,(r,s)}(Z, Y) = \sqrt{f_R \frac{hooks_R}{hooks_r hooks_s}} O_{R,(r,s)}(Z, Y)$$

In terms of these normalized operators

$$DO_{R,(r,s)}(Z, Y) = \sum_{T,(t,u)} N_{R,(r,s);T,(t,u)} O_{T,(t,u)}(Z, Y)$$

where

$$N_{R,(r,s);T,(t,u)} = 2g_{YM}^2 \sum_{R'} \frac{c_{RR'} d_T n m}{d_{R'} d_t d_u (n+m)} \sqrt{\frac{f_T hooks_T hooks_r hooks_s}{f_R hooks_R hooks_s hooks_u}}$$

$$Tr([\Gamma_R((n, n+1)), P_{R \rightarrow (r,s)}] I_{R'T'} [P_{T \rightarrow (t,u)}, \Gamma_T((n, n+1))] I_{T'R}) \quad (5.3)$$

Equation(5.3) will be used when the the spectrum of the dilatation operator is numerically studied in Chapter 7.

Chapter 6

Excited Giant Graviton Bound States

In this Chapter, the class of operators being studied will be defined as well as the approximations that can be made in the large N limit. In this thesis, restricted Schur Polynomials labelled by a Young Diagram with at most two columns will be studied. The number of Z s appearing will be αN where $2 - \alpha \equiv \zeta \ll 1$. The number of Y s appearing is fixed to $O(1)$. As previously mentioned, these operators are dual to giant gravitons that wrap an S^3 in the S^5 of the $AdS_5 \times S^5$ background. The restricted Schur Polynomials provide a suitable basis for the two giant system, that is, these operators capture all excitations (BPS and non supersymmetric) of the two giant system. The excitations of the single giant system using restricted Schur Polynomials was studied in [30]. The spacetime study of excitations of the single giant system using the Born-Infeld action can be seen in [48]. An important result from both [48] and [30] is that all deformations of the single threebrane giant gravitons that are in the $SU(2)$ sector are supersymmetric.

The mixing of these operators with restricted Schur Polynomials that

have three columns or more is suppressed by a factor $O(\frac{1}{\sqrt{N}})$. This factor comes from the normalization of the restricted Schur Polynomials. It was found in [30] that the three column restricted Schur Polynomial (with one short column) has a two point function which is smaller than the two column restricted Schur Polynomials by a factor $O(\frac{1}{N})$. Thus at large N , one need only study the two column restricted Schur Polynomials. This statement is the analog of the statement that for operators with dimension $O(1)$, different trace structures do not mix. The fact that the two column restricted Schur Polynomials are a decoupled sector at large N is to be expected. At large N , these operators correspond to a well defined stable semi classical object in spacetime namely the two giant system. It is expected that n column restricted Schur Polynomials are also a decoupled sector for the same reason.

Chapter 7

The Radial Direction

In this chapter, a limit in which the dilatation operator simplifies significantly will be discussed. There are only two columns in the Young Diagrams labeling the restricted Schur Polynomials. In the first column containing $O(\sqrt{N})$ more boxes than the second column, the dilatation operator simplifies to a lattice realization of the second derivative where the Young Diagram label defines the lattice.

7.1 Three Impurities

The three impurity operators are built using many Zs and three Ys. In order to specify these operators, the three Young Diagrams labelling the restricted Schur Polynomials must be given. The second Young diagram, r , is specified by stating the number of rows with two boxes ($=b_0$) and the number of rows containing a single box ($=b_1$). The third Young diagram label, s , and the first Young diagram label, R , can be built from r by specifying which boxes in R are to be removed to obtain r and how the boxes removed are to be assembled into s . Note that for this example, label R specifies an irreducible

brane giant gravitons with open strings stretched between them. Imposing the limits on the action of the dilatation operator expressions as seen in Appendix A, gives

$$\begin{aligned}
DO_A(b_0, b_1) &= g_{YM}^2(N - b_0) \times O\left(\frac{1}{b_1}\right) \\
DO_B(b_0, b_1) &= -\frac{4}{3}g_{YM}^2(N - b_0) \left[O_B(b_0 + 1, b_1 - 2) - 2O_B(b_0, b_1) \right. \\
&\quad \left. + O_B(b_0 - 1, b_1 + 2) \right] + \frac{2\sqrt{2}}{3}g_{YM}^2(N - b_0) \left[O_C(b_0 + 1, b_1 - 2) \right. \\
&\quad \left. - 2O_C(b_0 + 1, b_1) + O_C(b_0 - 1, b_1 + 2) \right] \\
DO_C(b_0, b_1) &= \frac{2\sqrt{2}}{3}g_{YM}^2(N - b_0) \left[O_B(b_0 + 1, b_1 - 2) - 2O_B(b_0, b_1) \right. \\
&\quad \left. + O_B(b_0 - 1, b_1 + 2) \right] - \frac{2}{3}g_{YM}^2(N - b_0) \left[O_C(b_0 + 1, b_1 - 2) \right. \\
&\quad \left. - 2O_C(b_0, b_1) + O_C(b_0 - 1, b_1 + 2) \right] \\
DO_D(b_0, b_1) &= -\frac{4}{3}g_{YM}^2(N - b_0) \left[O_D(b_0 + 1, b_1 - 2) - 2O_D(b_0, b_1) \right. \\
&\quad \left. + O_D(b_0 - 1, b_1 + 2) \right] + \frac{2\sqrt{2}}{3}g_{YM}^2(N - b_0) \left[O_E(b_0 + 1, b_1 - 2) \right. \\
&\quad \left. - 2O_E(b_0, b_1) + O_E(b_0 - 1, b_1 + 2) \right] \\
DO_E(b_0, b_1) &= \frac{2\sqrt{2}}{3}g_{YM}^2(N - b_0) \left[O_D(b_0 + 1, b_1 - 2) - 2O_D(b_0, b_1) \right. \\
&\quad \left. + O_D(b_0 - 1, b_1 + 2) \right] - \frac{2}{3}g_{YM}^2(N - b_0) \left[O_E(b_0 + 1, b_1 - 2) \right. \\
&\quad \left. - 2O_E(b_0, b_1) + O_E(b_0 - 1, b_1 + 2) \right] \\
DO_F(b_0, b_1) &= g_{YM}^2(N - b_0) \times O\left(\frac{1}{b_1}\right)
\end{aligned}$$

Firstly, notice that there are four operators for which the S_m representation is completely antisymmetric. It will be seen that there are also four

operators for which the corresponding states are also supersymmetric. In general for two giant systems, there will be an agreement between the number of totally antisymmetric representations of S_m and the number of supersymmetric states. By now considering the labels, $O_A(b_0, b_1)$ can be interpreted as being a state in which only the larger of the threebranes is deformed. From Chapter Five, it was discussed that deforming a single threebrane gives a supersymmetric state thus it is expected for $O_A(b_0, b_1)$ to remain supersymmetric. $O_F(b_0, b_1)$ can be interpreted in a similar way. For $O_F(b_0, b_1)$, it is the smaller threebrane which is deformed. Again, $O_F(b_0, b_1)$ will remain supersymmetric. Consider now the combinations of $O_B(b_0, b_1) + \sqrt{2}O_C(b_0, b_1)$ and $O_D(b_0, b_1) + \sqrt{2}O_E(b_0, b_1)$. Each combination of states is annihilated by D . This implies that there are another two supersymmetric ways to deform the threebrane. Finally, notice that if one set $O_B(b_0, b_1) - O_C(b_0, b_1)/\sqrt{2} \equiv O_{B-C}(b_0, b_1)$ and $O_D(b_0, b_1) - O_E(b_0, b_1)/\sqrt{2} \equiv O_{D-E}(b_0, b_1)$ then

$$\begin{aligned}
DO_{B-C}(b_0, b_1) &= -2g_{YM}^2(N - b_0) \left[O_{B-C}(b_0 + 1, b_1 - 2) \right. \\
&\quad \left. - 2O_{B-C}(b_0, b_1) + O_{B-C}(b_0 - 1, b_1 + 2) \right] \\
DO_{D-E}(b_0, b_1) &= -2g_{YM}^2(N - b_0) \left[O_{D-E}(b_0 + 1, b_1 - 2) \right. \\
&\quad \left. - 2O_{D-E}(b_0, b_1) + O_{D-E}(b_0 - 1, b_1 + 2) \right]
\end{aligned}$$

The right hand side is a discretization of the second derivative. The Young Diagram itself is defining the lattice. Note that if the number of boxes in each column sets the angular momentum and thus the radius of the threebrane (as the threebrane wraps S_3 of a given radius then it is this radius that is known as the ‘radius of the threebrane’), then it can be seen that the radius of the threebrane with the local physics in the radial direction has emerged.

$N-b_0=O(N)$, $b_0=O(N)$ and $b_1=O(\sqrt{N})$ will simplify the dynamics. When applying these limits the action of the dilatation operator becomes

$$\begin{aligned}
DO_A(b_0, b_1) &= (N - b_0)g_{YM}^2 \times O\left(\frac{1}{b_1}\right) \\
DO_B(b_0, b_1) &= -\frac{3}{2}g_{YM}^2(N - b_0) \left[O_B(b_0 + 1, b_1 - 2) - 2O_B(b_0, b_1) \right. \\
&\quad \left. + O_B(b_0 - 1, b_1 + 2) \right] + \frac{\sqrt{3}}{2}g_{YM}^2(N - b_0) \left[O_C(b_0 + 1, b_1 - 2) \right. \\
&\quad \left. - 2O_C(b_0 + 1, b_1) + O_C(b_0 - 1, b_1 + 2) \right] \\
DO_C(b_0, b_1) &= \frac{\sqrt{3}}{2}g_{YM}^2(N - b_0) \left[O_B(b_0 + 1, b_1 - 2) - 2O_B(b_0, b_1) \right. \\
&\quad \left. + O_B(b_0 - 1, b_1 + 2) \right] - \frac{1}{2}g_{YM}^2(N - b_0) \left[O_C(b_0 + 1, b_1 - 2) \right. \\
&\quad \left. - 2O_C(b_0, b_1) + O_C(b_0 - 1, b_1 + 2) \right] \\
DO_D(b_0, b_1) &= -2g_{YM}^2(N - b_0) \left[O_D(b_0 + 1, b_1 - 2) - 2O_D(b_0, b_1) \right. \\
&\quad \left. + O_D(b_0 - 1, b_1 + 2) \right] + \frac{2}{\sqrt{3}}g_{YM}^2(N - b_0) \left[O_E(b_0 + 1, b_1 - 2) \right. \\
&\quad \left. - 2O_E(b_0 + 1, b_1) + O_E(b_0 - 1, b_1 + 2) \right] \\
DO_E(b_0, b_1) &= -2g_{YM}^2(N - b_0) \left[O_E(b_0 + 1, b_1 - 2) - 2O_E(b_0, b_1) \right. \\
&\quad \left. + O_E(b_0 - 1, b_1 + 2) \right] + \frac{2}{\sqrt{3}}g_{YM}^2(N - b_0) \left[O_D(b_0 + 1, b_1 - 2) \right. \\
&\quad \left. - 2O_D(b_0, b_1) + O_D(b_0 - 1, b_1 + 2) \right] + \frac{2\sqrt{6}}{3}g_{YM}^2(N - b_0) \left[O_F(b_0 + 1, b_1 - 2) \right. \\
&\quad \left. - 2O_F(b_0, b_1) + O_F(b_0 - 1, b_1 + 2) \right]
\end{aligned}$$

$$\begin{aligned}
DO_F(b_0, b_1) &= -2g_{YM}^2 (N - b_0) \left[O_F(b_0 + 1, b_1 - 2) - 2O_F(b_0, b_1) \right. \\
&\quad \left. + O_F(b_0 - 1, b_1 + 2) \right] + \frac{2\sqrt{6}}{3} g_{YM}^2 (N - b_0) \left[O_E(b_0 + 1, b_1 - 2) \right. \\
&\quad \left. - 2O_E(b_0 + 1, b_1) + O_E(b_0 - 1, b_1 + 2) \right] \\
DO_G(b_0, b_1) &= -\frac{3}{2} g_{YM}^2 (N - b_0) \left[O_G(b_0 + 1, b_1 - 2) - 2O_G(b_0, b_1) \right. \\
&\quad \left. + O_G(b_0 - 1, b_1 + 2) \right] + \frac{\sqrt{3}}{2} g_{YM}^2 (N - b_0) \left[O_H(b_0 + 1, b_1 - 2) \right. \\
&\quad \left. - 2O_H(b_0 + 1, b_1) + O_H(b_0 - 1, b_1 + 2) \right] \\
DO_H(b_0, b_1) &= -\frac{1}{2} g_{YM}^2 (N - b_0) \left[O_H(b_0 + 1, b_1 - 2) - 2O_H(b_0, b_1) \right. \\
&\quad \left. + O_H(b_0 - 1, b_1 + 2) \right] + \frac{\sqrt{3}}{2} g_{YM}^2 (N - b_0) \left[O_G(b_0 + 1, b_1 - 2) \right. \\
&\quad \left. - 2O_G(b_0 + 1, b_1) + O_G(b_0 - 1, b_1 + 2) \right] \\
DO_I(b_0, b_1) &= (N - b_0) g_{YM}^2 \times O\left(\frac{1}{b_1}\right)
\end{aligned}$$

Again, it can be seen that the combinations of certain operators are annihilated by the action of D. These combinations of operators are $O_B(b_0, b_1) + \sqrt{3}O_C(b_0, b_1)$, $O_D(b_0, b_1) + \sqrt{3}O_E(b_0, b_1) + \sqrt{2}O_F(b_0, b_1)$ and $O_G(b_0, b_1) + \sqrt{3}O_H(b_0, b_1)$. For both the case of the three impurities and the the case of the four impurities, the following can be written for all the operators

$$O_{\text{BPS}}(R, r) = \sum_s \sqrt{d_s} O_{R,(r,s)}(b_0, b_1)$$

where d_s is the dimension of the irreducible representation s of the symmetric group. As was seen for the three impurity case, making the substitution $\sqrt{3}O_B(b_0, b_1) - O_C(b_0, b_1) \equiv O_{B-C}(b_0, b_1)$, $\sqrt{2}O_D(b_0, b_1) - O_F(b_0, b_1) \equiv$

$O_{D-F}(b_0, b_1)$, $O_D(b_0, b_1) - \sqrt{3}O_E(b_0, b_1) + \sqrt{2}O_F(b_0, b_1) \equiv O_{DF-E}(b_0, b_1)$ and $\sqrt{3}O_G(b_0, b_1) - O_H(b_0, b_1) \equiv O_{G-H}(b_0, b_1)$, results in the following

$$\begin{aligned}
DO_{B-C}(b_0, b_1) &= -2g_{YM}^2(N - b_0) \left[O_{B-C}(b_0 + 1, b_1 - 2) - 2O_{B-C}(b_0, b_1) \right. \\
&\quad \left. + O_{B-C}(b_0 - 1, b_1 + 2) \right] \\
DO_{D-F}(b_0, b_1) &= -2g_{YM}^2(N - b_0) \left[O_{D-F}(b_0 + 1, b_1 - 2) - 2O_{D-F}(b_0, b_1) \right. \\
&\quad \left. + O_{D-F}(b_0 - 1, b_1 + 2) \right] \\
DO_{DF-E}(b_0, b_1) &= -4g_{YM}^2(N - b_0) \left[O_{DF-E}(b_0 + 1, b_1 - 2) - 2O_{DF-E}(b_0, b_1) \right. \\
&\quad \left. + O_{DF-E}(b_0 - 1, b_1 + 2) \right] \\
DO_{G-H}(b_0, b_1) &= -2g_{YM}^2(N - b_0) \left[O_{G-H}(b_0 + 1, b_1 - 2) - 2O_{G-H}(b_0, b_1) \right. \\
&\quad \left. + O_{G-H}(b_0 - 1, b_1 + 2) \right]
\end{aligned}$$

Again, the right hand side is the discretization of the second derivative.

Chapter 8

Numerical Results

In this Chapter, the result of numerically diagonalizing the dilatation operator will be examined. In order to set up the numerical computation of the spectrum of the anomalous dimension, the maximum difference between the number of boxes in the the long column and the number of boxes in the short column must be specified. This value will be denoted a_{\max} . Given a_{\max} , the number of operators participating in the problem can be determined and it will also be possible to describe the resulting spectrum explicitly. The case where the difference between the number of boxes in the long column and the number of boxes in the short column is even will be considered (a_{\max} is even).

8.1 Two Impurities

For a given value of a_{\max} , there are $2+2a_{\max}$ states in total. Of the total number of states, $\frac{3}{2}a_{\max}+1$ values are zero eigenvalues and correspond to the supersymmetric states. The remaining values are

$$\lambda_i = 8g_{YM}^2 i \quad i = 1, 2, \dots, \frac{a_{\max}}{2} + 1.$$

8.2 Three Impurities

For a given value of a_{\max} , there are $1+3a_{\max}$ states in total. Of the total number of states, $2a_{\max}$ values are zero eigenvalues and correspond to the supersymmetric states. The remaining values are

$$\lambda_i = 8g_{YM}^2 i \quad i = 1, 2, \dots, \frac{a_{\max}}{2},$$

each with a degeneracy of two and a single maximum eigenvalue $\lambda = 4a_{\max}g_{YM}^2 + 8g_{YM}^2$. This degeneracy almost certainly indicates a symmetry enhancement in the large N limit.

8.3 Four Impurities

For a given value of a_{\max} , there are $1+\frac{9}{2}a_{\max}$ states in total. Of the total number of states, $\frac{5}{2}a_{\max}-1$ values are zero eigenvalues. Again, the eigenvalues are evenly spaced at $8g_{YM}^2$ and they are again degenerate. The low lying eigenvalues

$$\lambda_i = 8g_{YM}^2 i \quad i = 1, 2, \dots, \frac{a_{\max}}{2},$$

have a degeneracy which alternates between 3 and 4. Thus, there will be three eigenvalues $\lambda = 8g_{YM}^2$, then four eigenvalues $\lambda = 16g_{YM}^2$, then three eigenvalues $\lambda = 24g_{YM}^2$, then four eigenvalues $\lambda = 32g_{YM}^2$ and so on. If a_{\max} is a multiple of 4 then the larger eigenvalues are given by $\lambda = 4a_{\max}g_{YM}^2 + 8g_{YM}^2$, $\lambda = 4a_{\max}g_{YM}^2 + 16g_{YM}^2$ and

$$\lambda_i = 4a_{\max}g_{YM}^2 + 16g_{YM}^2 + 16ig_{YM}^2 \quad i = 1, 2, \dots, \frac{a_{\max}}{4}.$$

All of these larger eigenvalues are non-degenerate. If a_{\max} is not a multiple of 4 then the larger eigenvalues are given by $\lambda = 4a_{\max}g_{YM}^2 + 8g_{YM}^2$ with a

degeneracy of 2 and

$$\lambda_i = 4a_{\max}g_{YM}^2 + 16g_{YM}^2 + 16ig_{YM}^2 \quad i = 1, 2, \dots, \frac{a_{\max} + 2}{4}.$$

All of these larger eigenvalues are non-degenerate.

These degeneracies observed almost certainly indicate a symmetry enhancement in the large N limit.

Chapter 9

Discussion

9.1 Results Discussion

The one loop anomalous dimension of an operator built from $O(N)$ Zs and three or four Y “impurities” has been computed. Several comments can be made from the results obtained. Firstly, it can be seen that the results for the one loop dilatation operator (Appendix A) are complicated. This result is expected as many classes of Feynman diagrams are summed, not only the planar diagrams. It can also be seen that although the results for the one loop dilatation operator are complicated, the spectra for the one loop anomalous dimensions are simple. In order to obtain a problem that was numerically solvable, the value for a_{\max} was kept finite. In the large N limit, $a_{\max} = \zeta N$ goes to infinity. For the purpose of the rest of the discussion, the assumption will be made that the limit $a_{\max} \rightarrow \infty$ is used.

For the case of two impurities [30], it was found that there were three times as many zero eigenvalue states as there were positive eigenvalue states. There are $\frac{a_{\max}}{2}$ positive eigenvalue states with a constant energy level spacing $8g_{YM}^2$. An oscillator can be naturally associated from this with a set of $\sim \frac{a_{\max}}{2}$

with $8g_{YM}^2$ level spacing and one harmonic oscillator with $16g_{YM}^2$ level spacing. Looking at the four impurity states as seen in Chapter 7, section 2, it can be seen that there are five operators with impurities in the antisymmetric representation, three operators with impurities in the $\begin{array}{|c|} \hline \square \\ \hline \end{array}$ representation and one operator with impurities in the $\begin{array}{|c|c|} \hline \square & \square \\ \hline \end{array}$ representation. Although the frequencies of the harmonic oscillators have been obtained by considering the representations which organize the impurities, it does not mean that the claim is made (for example) that operators O_F correspond to the frequency $16g_{YM}^2$ operators.

It can be noted that the case for five impurities was not studied because the methods used break down but rather because as the number of impurities increase so does the level of difficulty and complication in writing down the projectors and computing the action of the dilatation operator. In principle there is no problem with considering an operator with $O(N)$ impurities. The case of no impurities and one impurity were computed in [30] analytically with the result that all the operators were annihilated by the one loop dilatation operator.

From the results obtained, it is possible to guess a result for a general number of impurities. Two general cases can be considered, the case with an even number of impurities and the case with an odd number of impurities. For the case of an even number of impurities $= 2n$ then one would expect a set of oscillators with frequency ω_i and degeneracy d_i of the form

$$\omega_i = 8ig_{YM}^2, \quad d_i = 2(n - i) + 1, \quad i = 0, 1, \dots, n.$$

For the case of an odd number of impurities $= 2n + 1$ then one would expect a set of oscillators with frequency ω_i and degeneracy d_i of the form

$$\omega_i = 8ig_{YM}^2, \quad d_i = 2(n - i + 1), \quad i = 0, 1, \dots, n.$$

This conjecture passes a counting test: $\sum_i d_i$ is equal to the number of Schur Polynomials that can be defined. Also, the number of degeneracies d_i match the number of each type of oscillator that can be defined. So d_i is equal to the number of operators with impurities organized into a Young diagram with i boxes in the short column.

Although the expressions obtained for the dilatation operator are rather complicated, the underlying picture is quite simple. The dilatation operator is equivalent to a set of harmonic oscillators. For each type of operator there is a single oscillator whose frequency is determined by the representation which arranges the impurities. As sets of harmonic oscillators are integrable systems, then the system studied is also an example of an integrable dilatation operator obtained by summing planar and non planar diagrams.

So far, the results have been discussed solely on the CFT side of the AdS/CFT correspondence. It is natural to consider the dual interpretation of the results. The operators considered are dual to giant gravitons. It was seen in [34, 35, 36] that there is a connection between the geometry of giant gravitons and harmonic oscillators. The work in these papers quantize the Moduli space of Mikhailov's giant gravitons. Therefore, a huge space of states is captured. This huge space of states connects to harmonic oscillators. As this thesis has focused on a two giant system, it is therefore known that the oscillators that have been captured are associated to the two giant system and the excitations of it. The results obtained in this thesis give a more refined statement as to how the harmonic oscillator enters. It could be asked if the set of operators examined include excitations (for example) of a two giant system plus a graviton. This, however, is a small perturbation of the two giant system, not an excitation of it. The graviton would be an excitation of spacetime. The states obtained in this thesis do not have such excitations.

States which would have this type of excitation would correspond to operators with a small third column, which have decoupled at large N . In a similar way that quantizing the possible excitation modes of a string results in one obtaining a set of harmonic oscillators, it could be said that the oscillators obtained in this thesis arose from the quantization of the possible excitation modes of a giant graviton.

By using the limit of the first column of the Young Diagram containing $O\sqrt{N}$ more boxes than the second column, it was found that the dilatation operator simplifies to the lattice realization of the second derivative. It was the Young Diagram that defined the lattice. As the number of boxes in each column sets the angular momentum and hence the radius of the threebrane, it is clear that the radius of the giant graviton together with the local physics in the radial direction has emerged. For the operators studied in this thesis, the number of lattice sites is $O(N)$ whereas the number of lattice sites for BMN loops is $O\sqrt{N}$.

9.2 Further Studies

There are many directions which one could follow for further research. Given the simplicity of the results obtained for the spectra of the one loop anomalous dimensions, it should be possible to construct an analytic solution. This is still under investigation [50]. Another aspect of this which could be studied is how the results are modified at higher loops. One could also study the case of $n > 2$ column restricted Schur Polynomials and more species of impurities. It could also be asked when and how simple systems are expected to emerge from multimatrix models. It is already known that for a single matrix model the planar limit is captured by the dynamics of N non interacting

non-relativistic fermions in an external potential. In this thesis, it has been argued that the large N limit of a class of operators dual to giant gravitons is captured by a collection of harmonic oscillators. Perhaps every semi-classical object in spacetime is associated with the emergence of a simple system in the large N limit of the corresponding class of operators in the field theory.

Appendix A

Dilatation Operator for Three or Four Impurities

In what follows $D\mathcal{O} \equiv g_{YM}^2 \hat{D}\mathcal{O}$ with D the one loop Dilatation operator.

A.1 Three Impurities

$$\begin{aligned}
\hat{D}O_A(b_0, b_1) = & \sqrt{(N - b_0 - b_1 - 2)(N - b_0 + 1)} \left[4b_1 \sqrt{\frac{b_1 + 4}{b_1 + 2}} \frac{1}{(b_1 + 2)(b_1 + 3)} O_B(b_0, b_1) \right. \\
& - 2 \sqrt{\frac{b_1 + 4}{b_1 + 2}} \sqrt{2} \frac{1}{(b_1 + 2)} O_C(b_0, b_1) + 8 \sqrt{\frac{(b_1 + 4)(b_1 + 1)}{(b_1 + 2)(b_1 + 3)}} \frac{1}{(b_1 + 3)(b_1 + 2)} O_D(b_0 - 1, b_1 + 2) \\
& + 2 \sqrt{\frac{(b_1 + 4)(b_1 + 1)}{(b_1 + 3)(b_1 + 2)}} \frac{\sqrt{2}}{(b_1 + 3)(b_1 + 2)} O_E(b_0 - 1, b_1 + 2) \left. \right] + (N - b_0 - b_1 - 2) \left[\frac{12}{(b_1 + 2)(b_1 + 3)} O_A(b_0, b_1) \right. \\
& \left. - 4 \frac{\sqrt{(b_1 + 1)(b_1 + 3)}(b_1 + 5)}{(b_1 + 3)^2(b_1 + 2)} O_B(b_0 - 1, b_1 + 2) + 2 \frac{\sqrt{(b_1 + 1)(b_1 + 3)}\sqrt{2}}{(b_1 + 3)^2} O_C(b_0 - 1, b_1 + 2) \right]
\end{aligned}$$

$$\hat{D}O_B(b_0, b_1) = \sqrt{(N - b_0 - b_1 - 1)(N - b_0)} \left[-\frac{4}{3} \sqrt{\frac{(b_1 + 2)(b_1 - 1)}{b_1(b_1 + 1)}} \frac{(b_1 - 2)(b_1 + 3)}{b_1(b_1 + 1)} O_B(b_0 + 1, b_1 - 2) \right]$$

$$\begin{aligned}
& + \frac{2}{3} \frac{b_1 + 3}{b_1} \sqrt{\frac{(b_1 + 2)(b_1 - 1)}{(b_1 + 1)b_1}} \sqrt{2} O_C(b_0 + 1, b_1 - 2) - \frac{32}{3} \frac{b_1^2 + 2b_1 - 3}{b_1(b_1 + 1)(b_1 + 2)^2} \sqrt{\frac{b_1 + 2}{b_1}} O_D(b_0, b_1) \\
& - \frac{2\sqrt{2}}{3} \sqrt{\frac{b_1 + 2}{b_1} \frac{(b_1 + 3)(3b_1 - 2)}{b_1(b_1 + 2)(b_1 + 1)}} O_E(b_0, b_1) + 8 \sqrt{\frac{(b_1 + 3)b_1}{(b_1 + 2)(b_1 + 1)}} \frac{1}{(b_1 + 1)(b_1 + 2)} O_F(b_0 - 1, b_1 + 2) \Big] \\
& + \sqrt{(N - b_0 - b_1 - 2)(N - b_0 + 1)} \left[\frac{2}{3} \sqrt{\frac{(b_1 + 4)(b_1 + 1)}{(b_1 + 2)(b_1 + 3)}} \frac{\sqrt{2}b_1}{(b_1 + 3)} O_C(b_0 - 1, b_1 + 2) \right. \\
& \quad \left. - \frac{4}{3} \sqrt{\frac{(b_1 + 4)(b_1 + 1)}{(b_1 + 3)(b_1 + 2)}} \frac{(b_1 + 5)b_1}{(b_1 + 3)(b_1 + 2)} O_B(b_0 - 1, b_1 + 2) \right. \\
& \quad \left. + 4 \sqrt{\frac{b_1 + 4}{b_1 + 2}} \frac{b_1}{(b_1 + 3)(b_1 + 2)} O_A(b_0, b_1) \right] + (N - b_0 - b_1 - 1) \left[-4 \sqrt{\frac{b_1 - 1}{b_1 + 1}} \frac{(b_1 + 3)}{(b_1 + 1)b_1} O_A(b_0 + 1, b_1 - 2) \right. \\
& \quad \left. + \frac{4}{3} \frac{(b_1 + 3)(b_1^3 + 5b_1^2 + 8b_1 - 12)}{(b_1 + 1)b_1(b_1 + 2)^2} O_B(b_0, b_1) - \frac{2\sqrt{2}}{3} \frac{(b_1^2 + 2b_1 - 4)(b_1 + 3)}{(b_1 + 1)(b_1 + 2)^2} O_C(b_0, b_1) \right. \\
& \quad \left. - \frac{8}{3} \sqrt{\frac{b_1 + 3}{b_1 + 1}} \frac{(b_1 + 4)b_1}{(b_1 + 2)^2(b_1 + 1)} O_D(b_0 - 1, b_1 + 2) + \frac{4}{3} \sqrt{2} \sqrt{\frac{b_1 + 3}{b_1 + 1}} \frac{b_1}{(b_1 + 2)^2} O_E(b_0 - 1, b_1 + 2) \right] \\
& + (N - b_0 + 1) \left[\frac{4}{3} \frac{(b_1 + 4)b_1^2}{(b_1 + 3)(b_1 + 2)^2} O_B(b_0, b_1) + \frac{8}{3} \frac{\sqrt{(b_1 + 1)(b_1 + 3)}b_1(b_1 + 4)}{(b_1 + 3)^2(b_1 + 2)^2} O_D(b_0 - 1, b_1 + 2) \right. \\
& \quad \left. - \frac{2}{3} \frac{\sqrt{2}(b_1 + 4)b_1}{(b_1 + 2)^2} O_C(b_0, b_1) + \frac{2}{3} \frac{\sqrt{2}\sqrt{(b_1 + 1)(b_1 + 3)}b_1(b_1 + 4)}{(b_1 + 3)^2(b_1 + 2)^2} O_E(b_0 - 1, b_1 + 2) \right]
\end{aligned}$$

$$\begin{aligned}
\hat{D}O_C(b_0, b_1) & = \sqrt{(N - b_0 - b_1 - 1)(N - b_0)} \left[\frac{2\sqrt{2}}{3} \sqrt{\frac{(b_1 + 2)(b_1 - 1)}{(b_1 + 1)b_1}} \frac{(b_1 - 2)}{b_1 + 1} O_B(b_0 + 1, b_1 - 2) \right. \\
& - \frac{2}{3} \sqrt{\frac{(b_1 + 2)(b_1 - 1)}{(b_1 + 1)b_1}} O_C(b_0 + 1, b_1 - 2) + \frac{2\sqrt{2}}{3} \sqrt{\frac{b_1 + 2}{b_1}} \frac{(b_1 - 1)(3b_1 + 8)}{(b_1 + 1)(b_1 + 2)^2} O_D(b_0, b_1) \\
& \left. - \frac{4}{3} \sqrt{\frac{b_1 + 2}{b_1}} \frac{1}{(b_1 + 1)(b_1 + 2)} O_E(b_0, b_1) + 2 \frac{\sqrt{(b_1 + 2)(b_1 + 3)(b_1 + 1)}b_1\sqrt{2}}{(b_1 + 1)^2(b_1 + 2)^2} O_F(b_0 - 1, b_1 + 2) \right] \\
& + \sqrt{(N - b_0 - b_1 - 2)(N - b_0 + 1)} \left[-2 \frac{\sqrt{(b_1 + 4)(b_1 + 2)}\sqrt{2}}{(b_1 + 2)^2} O_A(b_0, b_1) \right. \\
& \left. + \frac{2\sqrt{2}}{3} \sqrt{\frac{(b_1 + 4)(b_1 + 1)}{(b_1 + 3)(b_1 + 2)}} \frac{(b_1 + 5)}{(b_1 + 2)} O_B(b_0 - 1, b_1 + 2) - \frac{2}{3} \sqrt{\frac{(b_1 + 4)(b_1 + 1)}{(b_1 + 2)(b_1 + 3)}} O_C(b_0 - 1, b_1 + 2) \right]
\end{aligned}$$

$$\begin{aligned}
& + (N - b_0 - b_1 - 1) \left[2 \sqrt{\frac{b_1 - 1}{b_1 + 1}} \sqrt{2} \frac{1}{b_1 + 1} O_A(b_0 + 1, b_1 - 2) \right. \\
& - \frac{2\sqrt{2}}{3} \frac{(b_1^2 + 2b_1 - 4)(b_1 + 3)}{(b_1 + 1)(b_1 + 2)^2} O_B(b_0, b_1) + \frac{2}{3} \frac{b_1(b_1^2 + 2b_1 - 1)}{(b_1 + 1)(b_1 + 2)^2} O_C(b_0, b_1) \\
& \left. - \frac{2}{3} \sqrt{2} \sqrt{\frac{b_1 + 3}{b_1 + 1}} \frac{(b_1 + 4)b_1}{(b_1 + 2)^2(b_1 + 1)} O_D(b_0 - 1, b_1 + 2) + \frac{2}{3} \sqrt{\frac{b_1 + 3}{b_1 + 1}} \frac{b_1}{(b_1 + 2)^2} O_E(b_0 - 1, b_1 + 2) \right] \\
& + (N - b_0 + 1) \left[-\frac{2}{3} \frac{\sqrt{2}(b_1 + 4)b_1}{(b_1 + 2)^2} O_B(b_0, b_1) + \frac{2}{3} \frac{(b_1 + 4)(b_1 + 3)}{(b_1 + 2)^2} O_C(b_0, b_1) \right. \\
& \left. - \frac{4}{3} \frac{\sqrt{2}\sqrt{(b_1 + 1)(b_1 + 3)}(b_1 + 4)}{(b_1 + 3)(b_1 + 2)^2} O_D(b_0 - 1, b_1 + 2) - \frac{2}{3} \frac{\sqrt{(b_1 + 1)(b_1 + 3)}(b_1 + 4)}{(b_1 + 3)(b_1 + 2)^2} O_E(b_0 - 1, b_1 + 2) \right]
\end{aligned}$$

$$\begin{aligned}
\hat{D}O_D(b_0, b_1) & = \sqrt{(N - b_0 - b_1)(N - b_0 - 1)} \left[-\frac{4}{3} \sqrt{\frac{(b_1 + 1)(b_1 - 2)}{b_1(b_1 - 1)}} \frac{(b_1 - 3)(b_1 + 2)}{b_1(b_1 - 1)} O_D(b_0 + 1, b_1 - 2) \right. \\
& \left. + \frac{2}{3} \frac{(b_1 + 2)\sqrt{b_1(b_1 - 1)(b_1 + 1)(b_1 - 2)}\sqrt{2}}{b_1(b_1 - 1)^2} O_E(b_0 + 1, b_1 - 2) - 4 \frac{(b_1 + 2)\sqrt{b_1(b_1 - 2)}}{b_1^2(b_1 - 1)} O_F(b_0, b_1) \right] \\
& + \sqrt{(N - b_0 - b_1 - 1)(N - b_0)} \left[\frac{8}{b_1(b_1 + 1)} \sqrt{\frac{(b_1 + 2)(b_1 - 1)}{(b_1 + 1)b_1}} O_A(b_0 + 1, b_1 - 2) \right. \\
& + \frac{2\sqrt{2}}{3} \frac{\sqrt{b_1(b_1 + 2)}(b_1 - 1)(3b_1 + 8)}{(b_1 + 1)(b_1 + 2)^2 b_1} O_C(b_0, b_1) - \frac{32}{3} \frac{(b_1^2 + 2b_1 - 3)\sqrt{b_1(b_1 + 2)}}{(b_1 + 2)^2 b_1^2 (b_1 + 1)} O_B(b_0, b_1) \\
& - \frac{4}{3} \sqrt{\frac{b_1(b_1 + 3)}{(b_1 + 2)(b_1 + 1)}} \frac{(b_1 - 1)(b_1 + 4)}{(b_1 + 2)(b_1 + 1)} O_D(b_0 - 1, b_1 + 2) \\
& \left. + \frac{2}{3} \sqrt{\frac{b_1(b_1 + 3)}{(b_1 + 2)(b_1 + 1)}} \sqrt{2} \frac{(b_1 - 1)}{b_1 + 2} O_E(b_0 - 1, b_1 + 2) \right] + (N - b_0) \left[\frac{4}{3} \frac{(b_1 - 1)(b_1^3 + b_1^2 + 16)}{(b_1 + 1)b_1^2(b_1 + 2)} O_D(b_0, b_1) \right. \\
& + \frac{8}{3} \sqrt{\frac{b_1 - 1}{b_1 + 1}} \frac{b_1^2 - 4}{b_1^2(b_1 + 1)} O_B(b_0 + 1, b_1 - 2) - \frac{4}{3} \sqrt{2} \sqrt{\frac{b_1 - 1}{b_1 + 1}} \frac{b_1 + 2}{b_1^2} O_C(b_0 + 1, b_1 - 2) \\
& \left. - \frac{2\sqrt{2}}{3} \frac{(b_1^2 + 2b_1 - 4)(b_1 - 1)}{(b_1 + 1)b_1^2} O_E(b_0, b_1) + 4(b_1 - 1) \sqrt{\frac{b_1 + 3}{b_1 + 1}} \frac{1}{(b_1 + 2)(b_1 + 1)} O_F(b_0 - 1, b_1 + 2) \right] \\
& + (N - b_0 - b_1) \left[\frac{4}{3} \frac{(b_1 - 2)(b_1 + 2)^2}{(b_1 - 1)b_1^2} O_D(b_0, b_1) - \frac{2\sqrt{2}}{3} \frac{(b_1^2 - 4)}{b_1^2} O_E(b_0, b_1) \right]
\end{aligned}$$

$$\begin{aligned}
& -\frac{8}{3} \sqrt{\frac{(b_1+1)(b_1^2-4)}{(b_1-1)b_1^2(b_1-1)}} O_B(b_0+1, b_1-2) - \frac{2\sqrt{2}}{3} \sqrt{\frac{(b_1+1)(b_1^2-4)}{(b_1-1)b_1^2(b_1-1)}} O_C(b_0+1, b_1-2) \Big] \\
\hat{D}O_E(b_0, b_1) &= \sqrt{(N-b_0-b_1)(N-b_0-1)} \left[\frac{2\sqrt{2}}{3} \sqrt{\frac{(b_1+1)(b_1-2)(b_1-3)}{b_1(b_1-1)}} O_D(b_0+1, b_1-2) \right. \\
& - \frac{2}{3} \frac{\sqrt{b_1(b_1-1)(b_1+1)(b_1-2)}}{b_1(b_1-1)} O_E(b_0+1, b_1-2) + 2 \frac{\sqrt{2}\sqrt{b_1(b_1-2)}}{b_1^2} O_F(b_0, b_1) \Big] \\
& + \sqrt{(N-b_0-b_1-1)(N-b_0)} \left[2 \frac{\sqrt{2}\sqrt{(b_1+2)(b_1-1)(b_1+1)b_1}}{b_1^2(b_1+1)^2} O_A(b_0+1, b_1-2) \right. \\
& - \frac{4}{3} \frac{\sqrt{b_1(b_1+2)}}{(b_1+2)(b_1+1)b_1} O_C(b_0, b_1) - \frac{2\sqrt{2}}{3} \sqrt{b_1(b_1+2)} \frac{(b_1+3)(3b_1-2)}{(b_1+1)b_1^2(b_1+2)} O_B(b_0, b_1) \\
& + \frac{2}{3} \sqrt{\frac{b_1(b_1+3)}{(b_1+2)(b_1+1)}} \sqrt{2} \frac{b_1+4}{b_1+1} O_D(b_0-1, b_1+2) - \frac{2}{3} \sqrt{\frac{b_1(b_1+3)}{(b_1+1)(b_1+2)}} O_E(b_0-1, b_1+2) \Big] \\
& + (N-b_0) \left[-\frac{2\sqrt{2}}{3} \frac{(b_1^2+2b_1-4)(b_1-1)}{(b_1+1)b_1^2} O_D(b_0, b_1) \right. \\
& + \frac{2}{3} \frac{(b_1+2)(b_1^2+2b_1-1)}{(b_1+1)b_1^2} O_E(b_0, b_1) - 2 \sqrt{\frac{b_1+3}{b_1+1}} \sqrt{2} \frac{1}{b_1+1} O_F(b_0-1, b_1+2) \\
& + \frac{2}{3} \sqrt{2} \sqrt{\frac{b_1-1}{b_1+1}} \frac{b_1^2-4}{(b_1+1)b_1^2} O_B(b_0+1, b_1-2) - \frac{2}{3} \sqrt{\frac{b_1-1}{b_1+1}} \frac{b_1+2}{b_1^2} O_C(b_0+1, b_1-2) \Big] \\
& + (N-b_0-b_1) \left[\frac{2}{3} \frac{(b_1^2-3b_1+2)}{b_1^2} O_E(b_0, b_1) - \frac{2\sqrt{2}}{3} \frac{(b_1^2-4)}{b_1^2} O_D(b_0, b_1) \right. \\
& + \frac{4\sqrt{2}}{3} \frac{(b_1-2)\sqrt{(b_1+1)(b_1-1)}}{b_1^2(b_1-1)} O_B(b_0+1, b_1-2) + \frac{2}{3} \frac{(b_1-2)\sqrt{(b_1+1)(b_1-1)}}{b_1^2(b_1-1)} O_C(b_0+1, b_1-2) \Big]
\end{aligned}$$

$$\begin{aligned}
\hat{D}O_F(b_0, b_1) &= \sqrt{(N-b_0-b_1)(N-b_0-1)} \left[8 \frac{\sqrt{b_1(b_1-1)(b_1+1)(b_1-2)}}{b_1^2(b_1-1)^2} O_B(b_0+1, b_1-2) \right. \\
& + 2 \frac{\sqrt{2}\sqrt{b_1(b_1-1)(b_1+1)(b_1-2)}}{b_1^2(b_1-1)^2} O_C(b_0+1, b_1-2) - 4(b_1+2) \sqrt{\frac{b_1-2}{b_1}} \frac{1}{b_1(b_1-1)} O_D(b_0, b_1) \Big]
\end{aligned}$$

$$\begin{aligned}
& +2\sqrt{\frac{b_1-2}{b_1}}\sqrt{2}\frac{1}{b_1}O_E(b_0, b_1) \Big] +4\frac{(b_1-3)\sqrt{(b_1+1)(b_1-1)}(N-b_0-1)}{b_1(b_1-1)^2}O_D(b_0+1, b_1-2) \\
& -2\frac{\sqrt{(b_1+1)(b_1-1)}\sqrt{2}(N-b_0-1)}{(b_1-1)^2}O_E(b_0+1, b_1-2) +12\frac{N-b_0-1}{b_1(b_1-1)}O_F(b_0, b_1)
\end{aligned}$$

A.2 Four Impurities

$$\begin{aligned}
\hat{D}O_A(b_0, b_1) &= \sqrt{(N-b_0-b_1-3)(N-b_0+1)} \left[6\sqrt{\frac{b_1+5}{b_1+3}}\frac{b_1}{(b_1+4)(b_1+2)}O_B(b_0, b_1) \right. \\
& \quad \left. -2\sqrt{3}\sqrt{\frac{b_1+5}{b_1+3}}\frac{1}{b_1+2}O_C(b_0, b_1) +12\frac{\sqrt{(b_1+1)(b_1+5)}}{(b_1+3)(b_1+2)(b_1+4)}O_D(b_0-1, b_1+2) \right. \\
& \quad \left. +4\sqrt{3}\frac{\sqrt{(b_1+5)(b_1+1)}}{(b_1+3)(b_1+4)(b_1+2)}O_E(b_0-1, b_1+2) \right] + (N-b_0-b_1-3) \left[\frac{24}{(b_1+2)(b_1+4)}O_A(b_0, b_1) \right. \\
& \quad \left. -6\sqrt{\frac{b_1+1}{b_1+3}}\frac{b_1+6}{(b_1+2)(b_1+4)}O_B(b_0-1, b_1+2) +2\sqrt{3}\sqrt{\frac{b_1+1}{b_1+3}}\frac{1}{b_1+4}O_C(b_0-1, b_1+2) \right]
\end{aligned}$$

$$\begin{aligned}
\hat{D}O_B(b_0, b_1) &= \sqrt{(N-b_0-b_1-2)(N-b_0)} \left[\frac{\sqrt{3}}{2}\sqrt{(b_1+3)(b_1-1)}\frac{b_1+4}{b_1(b_1+1)}O_C(b_0+1, b_1-2) \right. \\
& \quad \left. -\frac{3}{2}\frac{\sqrt{(b_1+3)(b_1-1)}}{(b_1+1)(b_1+2)}\frac{(b_1+4)(b_1-2)}{b_1}O_B(b_0+1, b_1-2) +3\frac{(b_1+4)(b_1-1)(b_1-6)}{b_1(b_1+3)(b_1+2)^2}\sqrt{\frac{b_1+3}{b_1+1}}O_D(b_0, b_1) \right. \\
& \quad \left. -\sqrt{3}\frac{(b_1+4)(3b_1-2)}{b_1(b_1+2)^2}\sqrt{\frac{b_1+3}{b_1+1}}O_E(b_0, b_1) +\frac{2b_1(b_1+4)}{(b_1+1)(b_1+3)(b_1+2)^2}\left(9O_G(b_0-1, b_1+2) +\sqrt{3}O_H(b_0-1, b_1+2)\right) \right. \\
& \quad \left. +\sqrt{(N-b_0-b_1-3)(N-b_0+1)}\left[-\frac{3}{2}\sqrt{(b_1+5)(b_1+1)}\frac{b_1(b_1+6)}{(b_1+3)(b_1+2)(b_1+4)}O_B(b_0-1, b_1+2) \right. \right. \\
& \quad \left. \left. +\frac{\sqrt{3}}{2}\sqrt{(b_1+5)(b_1+1)}\frac{b_1}{(b_1+3)(b_1+4)}O_C(b_0-1, b_1+2) +6\sqrt{(b_1+5)(b_1+3)}\frac{b_1}{(b_1+2)(b_1+3)(b_1+4)}O_A(b_0, b_1)\right] \right. \\
& \quad \left. +(N-b_0-b_1-2)\left[-6\sqrt{\frac{b_1-1}{b_1+1}}\frac{b_1+4}{b_1(b_1+2)}O_A(b_0+1, b_1-2) +\frac{3}{2}\frac{(b_1^3+7b_1^2+22b_1-24)(b_1+4)}{b_1(b_1+2)^2(b_1+3)}O_B(b_0, b_1) \right. \right. \\
& \quad \left. \left. -\frac{\sqrt{3}}{2}\frac{(b_1^2+3b_1-6)(b_1+4)}{(b_1+2)^2(b_1+3)}O_C(b_0, b_1) -6\sqrt{\frac{b_1+3}{b_1+1}}\frac{b_1(b_1+5)(b_1+4)}{(b_1+2)^2(b_1+3)^2}O_D(b_0-1, b_1+2) \right. \right. \\
& \quad \left. \left. +\sqrt{12}\sqrt{(b_1+3)(b_1+1)}\frac{b_1(b_1+4)}{(b_1+3)^2(b_1+2)^2}O_E(b_0-1, b_1+2)\right] + (N-b_0+1)\left[\frac{3}{2}\frac{b_1^2(b_1+5)}{(b_1+2)(b_1+3)(b_1+4)}O_B(b_0, b_1) \right. \right.
\end{aligned}$$

$$-\frac{\sqrt{3}}{2} \frac{(b_1+5)b_1}{(b_1+2)(b_1+3)} O_C(b_0, b_1) + 3\sqrt{(b_1+3)(b_1+1)} \frac{b_1(b_1+5)}{(b_1+3)^2(b_1+4)(b_1+2)} O_D(b_0-1, b_1+2) \\ + \sqrt{3}\sqrt{(b_1+3)(b_1+1)} \frac{b_1(b_1+5)}{(b_1+3)^2(b_1+2)(b_1+4)} O_E(b_0-1, b_1+2) \Big]$$

$$\hat{D}O_C(b_0, b_1) = \sqrt{(N-b_0-b_1-2)(N-b_0)} \left[\frac{\sqrt{3}}{2} \sqrt{(b_1-1)(b_1+3)} \frac{b_1-2}{(b_1+1)(b_1+2)} O_B(b_0+1, b_1-2) \right. \\ - \frac{1}{2} \sqrt{(b_1+3)(b_1-1)} \frac{1}{b_1+1} O_C(b_0+1, b_1-2) + \frac{1}{\sqrt{3}} \sqrt{\frac{b_1+3}{b_1+1}} \frac{(b_1-1)(5b_1+18)}{(b_1+3)(b_1+2)^2} O_D(b_0, b_1) \\ + \sqrt{\frac{b_1+3}{b_1+1}} \frac{3b_1-2}{(b_1+2)^2} O_E(b_0, b_1) + 2\sqrt{3} \frac{b_1(b_1+4)}{(b_1+1)(b_1+2)^2(b_1+3)} O_G(b_0-1, b_1+2) \\ \left. - \frac{4\sqrt{6}}{3} \sqrt{\frac{b_1+3}{b_1+1}} \frac{1}{b_1+2} O_F(b_0, b_1) + 2 \frac{(3b_1^2+12b_1+8)}{(b_1+3)(b_1+1)(b_1+2)^2} O_H(b_0-1, b_1+2) \right] \\ + \sqrt{(N-b_0-b_1-3)(N-b_0+1)} \left[\frac{\sqrt{3}}{2} \sqrt{(b_1+5)(b_1+1)} \frac{b_1+6}{(b_1+3)(b_1+2)} O_B(b_0-1, b_1+2) \right. \\ \left. - \frac{1}{2} \frac{\sqrt{(b_1+5)(b_1+1)}}{(b_1+3)} O_C(b_0-1, b_1+2) - 2\sqrt{3} \frac{\sqrt{(b_1+5)(b_1+3)}}{(b_1+3)(b_1+2)} O_A(b_0, b_1) \right] + (N-b_0-b_1-2) \times \\ \times \left[\sqrt{\frac{b_1-1}{b_1+1}} \frac{2\sqrt{3}}{b_1+2} O_A(b_0+1, b_1-2) - \frac{\sqrt{3}}{2} \frac{(b_1^2+3b_1-6)(b_1+4)}{(b_1+2)^2(b_1+3)} O_B(b_0, b_1) + \frac{b_1^3+3b_1^2+10b_1+32}{2(b_1+2)^2(b_1+3)} O_C(b_0, b_1) \right. \\ - \frac{2}{\sqrt{3}} \sqrt{\frac{b_1+3}{b_1+1}} \frac{b_1(b_1+5)(b_1+4)}{(b_1+2)^2(b_1+3)^2} O_D(b_0-1, b_1+2) - 2\sqrt{(b_1+3)(b_1+1)} \frac{(b_1+4)^2}{(b_1+2)^2(b_1+3)^2} O_E(b_0-1, b_1+2) \\ + \frac{4\sqrt{2}}{\sqrt{3}} \frac{\sqrt{(b_1+3)(b_1+1)}}{(b_1+2)(b_1+3)} O_F(b_0-1, b_1+2) \Big] + (N-b_0+1) \left[-\frac{\sqrt{3}}{2} \frac{b_1(b_1+5)}{(b_1+2)(b_1+3)} O_B(b_0, b_1) \right. \\ + \frac{1}{2} \frac{(b_1+5)(b_1+4)}{(b_1+2)(b_1+3)} O_C(b_0, b_1) - \sqrt{3}\sqrt{(b_1+3)(b_1+1)} \frac{b_1+5}{(b_1+3)^2(b_1+2)} O_D(b_0-1, b_1+2) \\ \left. - \sqrt{(b_1+3)(b_1+1)} \frac{(b_1+5)}{(b_1+2)(b_1+3)^2} O_E(b_0-1, b_1+2) \right]$$

$$\hat{D}O_D(b_0, b_1) = \sqrt{(N-b_0-b_1-1)(N-b_0-1)} \left[-2 \frac{(b_1^2-9)(b_1^2-4)}{b_1^2(b_1^2-1)} O_D(b_0+1, b_1-2) \right. \\ \left. + \frac{(b_1^2-4)(b_1+3)}{b_1^2(b_1+1)^2} \left[\frac{2(b_1+1)^2}{\sqrt{3}(b_1-1)} O_E(b_0+1, b_1-2) - \sqrt{\frac{b_1+1}{b_1-1}} \left(6O_G(b_0, b_1) + \frac{2}{\sqrt{3}} O_H(b_0, b_1) \right) \right] \right]$$

$$\begin{aligned}
& +3\sqrt{\frac{b_1-1}{b_1+1}} \frac{b_1^2+b_1-6}{b_1(b_1+1)(b_1+2)} O_G(b_0, b_1) - \sqrt{3}\sqrt{\frac{b_1-1}{b_1+1}} \frac{b_1+3}{b_1(b_1+1)} O_H(b_0, b_1) \\
& + 12\sqrt{\frac{(b_1+3)(b_1-1)}{b_1(b_1+1)(b_1+2)}} O_I(b_0-1, b_1+2) \Big] + \sqrt{(N-b_0-b_1-2)(N-b_0)} \times \\
& \times \left[-3\sqrt{(b_1+3)(b_1+1)} \frac{(b_1+4)(b_1-1)}{(b_1+1)^2 b_1(b_1+2)} O_B(b_0, b_1) + \sqrt{3}\sqrt{(b_1+3)(b_1+1)} \frac{b_1-1}{(b_1+1)^2(b_1+2)} O_C(b_0, b_1) \right. \\
& + 12\sqrt{\frac{(b_1+3)(b_1-1)}{b_1(b_1+1)(b_1+2)}} O_A(b_0+1, b_1-2) - 2\frac{b_1(b_1-1)(b_1+4)(b_1+5)}{(b_1+1)(b_1+3)(b_1+2)^2} O_D(b_0-1, b_1+2) \\
& + 6\sqrt{\frac{b_1+1}{b_1+3}} \frac{b_1(b_1^2+3b_1-4)}{(b_1+2)^2(b_1+1)^2} O_B(b_0, b_1) + \frac{2}{\sqrt{3}}\sqrt{\frac{b_1+1}{b_1+3}} \frac{b_1(b_1^2+3b_1-4)}{(b_1+2)^2(b_1+1)^2} O_C(b_0, b_1) \\
& + \frac{2}{\sqrt{3}} \frac{b_1(b_1+4)(b_1-1)}{(b_1+3)(b_1+2)^2} O_E(b_0-1, b_1+2) \Big] + (N-b_0-b_1-1) \left[-6\sqrt{\frac{b_1-1}{b_1+1}} \frac{b_1^3+3b_1^2-4b_1-12}{b_1^2(b_1^2-1)} O_B(b_0+1, b_1-2) \right. \\
& - \frac{2}{\sqrt{3}}\sqrt{\frac{b_1-1}{b_1+1}} \frac{b_1^3+3b_1^2-4b_1-12}{b_1^2(b_1^2-1)} O_C(b_0+1, b_1-2) + 2\frac{(b_1-2)(b_1+3)^2(b_1+2)}{b_1^2(b_1+1)^2} O_D(b_0, b_1) \\
& - \frac{2}{\sqrt{3}} \frac{(b_1-2)(b_1+3)(b_1-1)(b_1+2)}{b_1^2(b_1+1)^2} O_E(b_0, b_1) \Big] + (N-b_0) \left[3\sqrt{\frac{b_1-1}{b_1+1}} \frac{b_1^2+b_1-6}{b_1(b_1+1)(b_1+2)} O_B(b_0+1, b_1-2) \right. \\
& - \sqrt{3}\sqrt{\frac{b_1-1}{b_1+1}} \frac{b_1+3}{b_1(b_1+1)} O_C(b_0+1, b_1-2) + 6\frac{(b_1+3)(b_1-1)}{b_1(b_1+2)(b_1+1)^2} O_D(b_0, b_1) \\
& + 2\sqrt{3}\frac{(b_1+3)(b_1-1)}{(b_1+2)b_1(b_1+1)^2} O_E(b_0, b_1) \Big] + (N-b_0-b_1-1) \left[6\frac{(b_1+3)(b_1-1)}{(b_1+1)^2 b_1(b_1+2)} O_D(b_0, b_1) \right. \\
& + 2\sqrt{3}\frac{(b_1-1)(b_1+3)}{(b_1+1)^2 b_1(b_1+2)} O_E(b_0, b_1) - 3\sqrt{\frac{b_1+3}{b_1+1}} \frac{b_1^2+3b_1-4}{b_1(b_1+1)(b_1+2)} O_G(b_0-1, b_1+2) \\
& + \sqrt{3}\sqrt{\frac{b_1+3}{b_1+1}} \frac{(b_1-1)}{(b_1+1)(b_1+2)} O_H(b_0-1, b_1+2) \Big] + (N-b_0) \left[2\frac{(b_1+4)(b_1-1)^2 b_1}{(b_1+1)^2(b_1+2)^2} O_D(b_0, b_1) \right. \\
& - \frac{2}{\sqrt{3}} \frac{(b_1-1)(b_1+3)b_1(b_1+4)}{(b_1+1)^2(b_1+2)^2} O_E(b_0, b_1) + 6\sqrt{\frac{b_1+3}{b_1+1}} \frac{(b_1^2+3b_1-4)b_1}{(b_1+1)(b_1+2)^2(b_1+3)} O_G(b_0-1, b_1+2) \\
& \left. + \frac{2}{\sqrt{3}}\sqrt{\frac{b_1+3}{b_1+1}} \frac{(b_1^2+3b_1-4)b_1}{(b_1+1)(b_1+2)^2(b_1+3)} O_H(b_0-1, b_1+2) \right]
\end{aligned}$$

$$\begin{aligned}
\hat{D}O_E(b_0, b_1) &= \sqrt{(N-b_0-b_1-1)(N-b_0-1)} \left[\frac{2}{\sqrt{3}} \frac{b_1^3-3b_1^2-4b_1+12}{(b_1+1)b_1^2} O_D(b_0+1, b_1-2) \right. \\
& - 2\frac{(b_1^2-4)}{b_1^2} O_E(b_0+1, b_1-2) + \frac{2\sqrt{6}}{3} \frac{b_1+2}{b_1} O_F(b_0+1, b_1-2) + \sqrt{3}\sqrt{\frac{b_1-1}{b_1+1}} \frac{(b_1-2)(3b_1+8)}{b_1^2(b_1+2)} O_G(b_0, b_1)
\end{aligned}$$

$$\begin{aligned}
& -\sqrt{\frac{b_1-1}{b_1+1}} \frac{3b_1+8}{b_1^2} O_H(b_0, b_1) + 4\sqrt{3} \frac{\sqrt{(b_1+3)(b_1-1)}}{b_1(b_1+1)(b_1+2)} O_I(b_0-1, b_1+2) \Big] \\
& + \sqrt{(N-b_0-b_1-2)(N-b_0)} \left[-\sqrt{3} \sqrt{(b_1+1)(b_1+3)} \frac{(b_1+4)(b_1-1)}{b_1(b_1+1)^2(b_1+2)} O_B(b_0, b_1) \right. \\
& + \sqrt{(b_1+1)(b_1+3)} \frac{b_1-1}{(b_1+2)(b_1+1)^2} O_C(b_0, b_1) + 4\sqrt{3} \frac{\sqrt{(b_1-1)(b_1+3)}}{b_1(b_1+1)(b_1+2)} O_A(b_0+1, b_1-2) \\
& \quad - 2\sqrt{3} \sqrt{(b_1+3)(b_1+1)} \frac{b_1(b_1+4)}{(b_1+1)^2(b_1+2)^2} O_B(b_0, b_1) \\
& + 2\sqrt{(b_1+1)(b_1+3)} \frac{b_1^2}{(b_1+2)^2(b_1+1)^2} O_C(b_0, b_1) + \frac{2}{\sqrt{3}} \frac{b_1(b_1^2+9b_1+20)}{(b_1+1)(b_1+2)^2} O_D(b_0-1, b_1+2) \\
& \quad \left. - 2 \frac{b_1(b_1+4)}{(b_1+2)^2} O_E(b_0-1, b_1+2) + \frac{2\sqrt{2}}{\sqrt{3}} \frac{b_1}{(b_1+2)} O_F(b_0-1, b_1+2) \right] + (N-b_0-b_1-1) \times \\
& \times \left[2\sqrt{3} \sqrt{\frac{b_1-1}{b_1+1}} \frac{b_1^2-4}{b_1^2(b_1+1)} O_B(b_0+1, b_1-2) - 2\sqrt{\frac{b_1-1}{b_1+1}} \frac{(b_1+2)^2}{b_1^2(b_1+1)} O_C(b_0+1, b_1-2) \right. \\
& \quad - \frac{2}{\sqrt{3}} \frac{(b_1-2)(b_1+3)(b_1-1)(b_1+2)}{b_1^2(b_1+1)^2} O_D(b_0, b_1) + 2 \frac{(b_1^4+2b_1^3+b_1^2-4)}{b_1^2(b_1+1)^2} O_E(b_0, b_1) \\
& \quad \left. - \frac{2\sqrt{6}}{3} \frac{b_1^2+b_1-2}{b_1(b_1+1)} O_F(b_0, b_1) \right] + (N-b_0) \left[\sqrt{3} \sqrt{\frac{b_1-1}{b_1+1}} \frac{b_1^2+b_1-6}{(b_1+2)b_1(b_1+1)} O_B(b_0+1, b_1-2) \right. \\
& \quad - \sqrt{\frac{b_1-1}{b_1+1}} \frac{b_1+3}{b_1(b_1+1)} O_C(b_0+1, b_1-2) + 2\sqrt{3} \frac{(b_1+3)(b_1-1)}{b_1(b_1+2)(b_1+1)^2} O_D(b_0, b_1) \\
& + 2 \frac{(b_1+3)(b_1-1)}{b_1(b_1+2)(b_1+1)^2} O_E(b_0, b_1) \Big] + (N-b_0-b_1-1) \left[2\sqrt{3} \frac{(b_1-1)(b_1+3)}{(b_1+1)^2(b_1+2)b_1} O_D(b_0, b_1) \right. \\
& \quad + 2 \frac{(b_1+3)(b_1-1)}{(b_1+1)^2 b_1(b_1+2)} O_E(b_0, b_1) - \sqrt{3} \sqrt{\frac{b_1+3}{b_1+1}} \frac{b_1^2+3b_1-4}{b_1(b_1+1)(b_1+2)} O_G(b_0-1, b_1+2) \\
& + \sqrt{\frac{b_1+3}{b_1+1}} \frac{b_1-1}{(b_1+1)(b_1+2)} O_H(b_0-1, b_1+2) \Big] + (N-b_0) \left[-\frac{2}{\sqrt{3}} \frac{(b_1-1)(b_1+3)b_1(b_1+4)}{(b_1+1)^2(b_1+2)^2} O_D(b_0, b_1) \right. \\
& \quad + 2 \frac{(b_1+3)(b_1^2+3b_1+4)b_1}{(b_1+1)^2(b_1+2)^2} O_E(b_0, b_1) - \frac{2\sqrt{6}}{3} \frac{(b_1+3)b_1}{(b_1+2)(b_1+1)} O_F(b_0, b_1) \\
& \quad \left. - 2\sqrt{3} \sqrt{\frac{b_1+3}{b_1+1}} \frac{(b_1+4)b_1}{(b_1+1)(b_1+2)^2} O_G(b_0-1, b_1+2) + 2\sqrt{\frac{b_1+3}{b_1+1}} \frac{b_1^2}{(b_1+2)^2(b_1+1)} O_H(b_0-1, b_1+2) \right]
\end{aligned}$$

$$\hat{D}O_F(b_0, b_1) = \sqrt{(N-b_0-b_1-1)(N-b_0-1)} \left[\frac{2\sqrt{6}}{3} \frac{b_1-2}{b_1} O_E(b_0+1, b_1-2) - 2O_F(b_0+1, b_1-2) \right]$$

$$\begin{aligned}
& + \frac{4\sqrt{6}}{3} \frac{\sqrt{(b_1-1)(b_1+1)}}{b_1(b_1+1)} O_H(b_0, b_1) \Big] + \sqrt{(N-b_0-b_1-2)(N-b_0)} \Big[-2O_F(b_0-1, b_1+2) \\
& \frac{2\sqrt{2}}{\sqrt{3}} \frac{b_1+4}{b_1+2} O_E(b_0-1, b_1+2) - \frac{4\sqrt{6}}{3} \sqrt{\frac{b_1+3}{b_1+1}} \frac{1}{b_1+2} O_C(b_0, b_1) \Big] + (N-b_0-b_1-1) \times \\
& \times \left[\frac{4\sqrt{6}}{3} \sqrt{\frac{b_1-1}{b_1+1}} \frac{1}{b_1} O_C(b_0+1, b_1-2) - \frac{2\sqrt{6}}{3} \frac{b_1^2+b_1-2}{b_1(b_1+1)} O_E(b_0, b_1) + 2 \frac{b_1-1}{b_1+1} O_F(b_0, b_1) \right] \\
& + (N-b_0) \left[-\frac{2\sqrt{6}}{3} \frac{(b_1+3)b_1}{(b_1+2)(b_1+1)} O_E(b_0, b_1) + 2 \frac{(b_1+3)}{b_1+1} O_F(b_0, b_1) - \frac{4\sqrt{6}}{3} \sqrt{\frac{b_1+3}{b_1+1}} \frac{1}{b_1+2} O_H(b_0-1, b_1+2) \right]
\end{aligned}$$

$$\begin{aligned}
\hat{D}O_G(b_0, b_1) &= \sqrt{(N-b_0-b_1)(N-b_0-2)} \left[-\frac{3}{2} \frac{\sqrt{(b_1+1)(b_1-3)}(b_1^2-2b_1-8)}{b_1(b_1-2)(b_1-1)} O_G(b_0+1, b_1-2) \right. \\
& + \frac{\sqrt{3}}{2} \frac{\sqrt{(b_1+1)(b_1-3)}(b_1+2)}{(b_1-2)(b_1-1)} O_H(b_0+1, b_1-2) - 6\sqrt{\frac{b_1-3}{b_1-1}} \frac{(b_1+2)}{b_1(b_1-2)} O_I(b_0, b_1) \Big] \\
& + \sqrt{(N-b_0-b_1-1)(N-b_0-1)} \left[18 \frac{(b_1^2-4)}{b_1^2(b_1^2-1)} O_B(b_0+1, b_1-2) \right. \\
& + 2\sqrt{3} \frac{(b_1^2-4)}{b_1^2(b_1^2-1)} O_C(b_0+1, b_1-2) - 3\sqrt{\frac{b_1-1}{b_1+1}} \frac{(b_1-2)(b_1+8)(b_1+3)}{b_1^2(b_1+2)(b_1-1)} O_D(b_0, b_1) \\
& + \sqrt{3} \sqrt{\frac{b_1-1}{b_1+1}} \frac{(b_1-2)(3b_1+8)}{b_1^2(b_1+2)} O_E(b_0, b_1) - \frac{3}{2} \sqrt{(b_1+3)(b_1-1)} \frac{(b_1^2+2b_1-8)}{b_1(b_1+1)(b_1+2)} O_G(b_0-1, b_1+2) \\
& + \frac{\sqrt{3}}{2} \sqrt{(b_1+3)(b_1-1)} \frac{(b_1-2)}{(b_1+1)(b_1+2)} O_H(b_0-1, b_1+2) \Big] + (N-b_0-b_1) \left[-\frac{\sqrt{3}}{2} \frac{b_1^2-b_1-6}{b_1(b_1-1)} O_H(b_0, b_1) \right. \\
& - \sqrt{3} \sqrt{(b_1+1)(b_1-1)} \frac{b_1^2-b_1-6}{(b_1-2)(b_1-1)^2 b_1} O_E(b_0+1, b_1-2) + \frac{3}{2} \frac{(b_1-3)(b_1+2)^2}{b_1(b_1-2)(b_1-1)} O_G(b_0, b_1) \\
& \left. - 3\sqrt{\frac{b_1+1}{b_1-1}} \frac{b_1^2-b_1-6}{(b_1-2)(b_1-1)b_1} O_D(b_0+1, b_1-2) \right] + (N-b_0-1) \left[-\frac{\sqrt{3}}{2} \frac{(b_1-2)(b_1^2+b_1-8)}{b_1^2(b_1-1)} O_H(b_0, b_1) \right. \\
& + \frac{3}{2} \frac{(b_1-2)(b_1^3-b_1^2+6b_1+48)}{b_1^2(b_1-1)(b_1+2)} O_G(b_0, b_1) + 6\sqrt{\frac{b_1-1}{b_1+1}} \frac{(b_1-2)(b_1-3)(b_1+2)}{b_1^2(b_1-1)^2} O_D(b_0+1, b_1-2) \\
& \left. - 2\sqrt{3} \sqrt{(b_1+1)(b_1-1)} \frac{b_1^2-4}{(b_1-1)^2 b_1^2} O_E(b_0+1, b_1-2) + 6\sqrt{\frac{b_1+3}{b_1+1}} \frac{(b_1-2)}{b_1(b_1+2)} O_I(b_0-1, b_1+2) \right]
\end{aligned}$$

$$\hat{D}O_H(b_0, b_1) = \sqrt{(N-b_0-b_1)(N-b_0-2)} \left[\frac{\sqrt{3}}{2} \frac{\sqrt{(b_1+1)(b_1-3)}(b_1-4)}{(b_1-1)b_1} O_G(b_0+1, b_1-2) \right]$$

$$\begin{aligned}
& \left. -\frac{1}{2} \frac{\sqrt{(b_1+1)(b_1-3)}}{b_1-1} O_H(b_0+1, b_1-2) + 2\sqrt{3} \frac{\sqrt{(b_1-1)(b_1-3)}}{b_1(b_1-1)} O_I(b_0, b_1) \right] \\
& + \sqrt{(N-b_0-b_1-1)(N-b_0-1)} \left[2\sqrt{3} \frac{b_1^2-4}{b_1^2(b_1^2-1)} O_B(b_0+1, b_1-2) \right. \\
& + 2\frac{3b_1^2-4}{b_1^2(b_1^2-1)} O_C(b_0+1, b_1-2) - \frac{2}{\sqrt{3}} \sqrt{\frac{b_1-1}{b_1+1}} \frac{b_1^3+3b_1^2-4b_1-12}{(b_1^2-1)b_1^2} O_D(b_0, b_1) \\
& - 2\sqrt{\frac{b_1-1}{b_1+1}} \frac{(b_1+2)^2}{b_1^2(b_1+1)} O_E(b_0, b_1) + \frac{4\sqrt{6}}{3} \sqrt{\frac{b_1-1}{b_1+1}} \frac{1}{b_1} O_F(b_0, b_1) \\
& \left. + \sqrt{\frac{b_1-1}{b_1+1}} \frac{b_1+3}{b_1(b_1+1)} \left(-\sqrt{3} O_D(b_0, b_1) - O_E(b_0, b_1) \right) \right] \\
& + \frac{\sqrt{3}}{2} \sqrt{(b_1+3)(b_1-1)} \frac{b_1+4}{b_1(b_1+1)} O_G(b_0-1, b_1+2) - \frac{1}{2} \sqrt{(b_1+3)(b_1-1)} \frac{1}{b_1+1} O_H(b_0-1, b_1+2) \Big] \\
& + (N-b_0-b_1) \left[\sqrt{3} \sqrt{\frac{b_1+1}{b_1-1}} \frac{(b_1-3)}{b_1(b_1-1)} O_D(b_0+1, b_1-2) + \sqrt{\frac{b_1+1}{b_1-1}} \frac{b_1-3}{b_1(b_1-1)} O_E(b_0+1, b_1-2) \right. \\
& \left. - \frac{\sqrt{3}}{2} \frac{b_1^2-b_1-6}{b_1(b_1-1)} O_G(b_0, b_1) + \frac{1}{2} \frac{b_1^2-5b_1+6}{b_1(b_1-1)} O_H(b_0, b_1) \right] + (N-b_0-1) \times \\
& \times \left[\frac{2}{\sqrt{3}} \sqrt{\frac{b_1-1}{b_1+1}} \frac{b_1^3-3b_1^2-4b_1+12}{b_1^2(b_1-1)^2} O_D(b_0+1, b_1-2) + 2 \frac{(b_1^2-4b_1+4)\sqrt{(b_1+1)(b_1-1)}}{b_1^2(b_1-1)^2} O_E(b_0+1, b_1-2) \right. \\
& - \frac{4\sqrt{6}}{3} \frac{\sqrt{(b_1+1)(b_1-1)}}{b_1(b_1-1)} O_F(b_0+1, b_1-2) - \frac{\sqrt{3}}{2} \frac{(b_1-2)(b_1^2+b_1-8)}{b_1^2(b_1-1)} O_G(b_0, b_1) \\
& \left. + \frac{b_1^3+3b_1^2+10b_1-16}{2b_1^2(b_1-1)} O_H(b_0, b_1) - 2\sqrt{3} \sqrt{\frac{b_1+3}{b_1+1}} \frac{1}{b_1} O_I(b_0-1, b_1+2) \right]
\end{aligned}$$

$$\begin{aligned}
\hat{D}O_I(b_0, b_1) &= \sqrt{(N-b_0-b_1)(N-b_0-2)} \left[12\sqrt{(b_1+1)(b_1-3)} \frac{1}{b_1(b_1-2)(b_1-1)} O_D(b_0+1, b_1-2) \right. \\
& + 4\sqrt{3} \sqrt{\frac{(b_1+1)(b_1-3)}{b_1(b_1-1)(b_1-2)}} O_E(b_0+1, b_1-2) - 6\sqrt{\frac{b_1-3}{b_1-1}} \frac{b_1+2}{b_1(b_1-2)} O_G(b_0, b_1) \\
& \left. + 2\sqrt{3} \sqrt{\frac{b_1-3}{b_1-1}} \frac{1}{b_1} O_H(b_0, b_1) \right] + (N-b_0-2) \left[6 \frac{\sqrt{(b_1+1)(b_1-1)(b_1-4)}}{b_1(b_1-1)(b_1-2)} O_G(b_0+1, b_1-2) \right. \\
& \left. - 2\sqrt{3} \frac{\sqrt{(b_1+1)(b_1-1)}}{(b_1-2)(b_1-1)} O_H(b_0+1, b_1-2) + 24 \frac{1}{b_1(b_1-2)} O_I(b_0, b_1) \right]
\end{aligned}$$

Appendix B

Intertwiners

When S^n acts on $V^{\otimes n}$ $n > 1$ it furnishes a reducible representation. Imagine that this includes the irreducible representations R and S . Representing the action of σ as a matrix $\Gamma(\sigma)$, in a suitable basis we can write

$$\Gamma(\sigma) = \begin{bmatrix} \Gamma_R(\sigma) & 0 & \cdots \\ 0 & \Gamma_S(\sigma) & \cdots \\ \cdots & \cdots & \cdots \end{bmatrix}.$$

If we restrict our selves to an S_{n-1} subgroup of S_n , then in general, both R and S will subduce a number of representations. Assume for the sake of this discussion that R subduces R'_1 and R'_2 and that S subduces S'_1 and S'_2 . Then, for $\sigma \in S_{n-1}$ we have

$$\Gamma(\sigma) = \begin{bmatrix} \Gamma_{R'_1}(\sigma) & 0 & 0 & 0 & \cdots \\ 0 & \Gamma_{R'_2}(\sigma) & 0 & 0 & \cdots \\ 0 & 0 & \Gamma_{S'_1}(\sigma) & 0 & \cdots \\ 0 & 0 & 0 & \Gamma_{S'_2}(\sigma) & \cdots \\ \cdots & \cdots & \cdots & \cdots & \cdots \end{bmatrix}.$$

Imagine that $S'_1 = R'_1$, that is, one of the irreducible representations

subduced by R is also subduced by S . Then, a simple application of the fundamental orthogonality relation gives

$$\begin{aligned}
& \sum_{\sigma \in S_{n-1}} \left[\begin{array}{ccccc} \Gamma_{R'_1}(\sigma) & 0 & 0 & 0 & \cdots \\ 0 & 0 & 0 & 0 & \cdots \\ 0 & 0 & 0 & 0 & \cdots \\ 0 & 0 & 0 & 0 & \cdots \\ \cdots & \cdots & \cdots & \cdots & \cdots \end{array} \right]_{ij} \left[\begin{array}{ccccc} 0 & 0 & 0 & 0 & \cdots \\ 0 & 0 & 0 & 0 & \cdots \\ 0 & 0 & \Gamma_{S'_1}(\sigma) & 0 & \cdots \\ 0 & 0 & 0 & 0 & \cdots \\ \cdots & \cdots & \cdots & \cdots & \cdots \end{array} \right]_{ab} \\
&= \frac{(n-1)!}{d_{R'_1}} \delta_{R'_1 S'_1} \left[\begin{array}{ccccc} 0 & 0 & \mathbf{1} & 0 & \cdots \\ 0 & 0 & 0 & 0 & \cdots \\ 0 & 0 & 0 & 0 & \cdots \\ 0 & 0 & 0 & 0 & \cdots \\ \cdots & \cdots & \cdots & \cdots & \cdots \end{array} \right]_{ib} \left[\begin{array}{ccccc} 0 & 0 & 0 & 0 & \cdots \\ 0 & 0 & 0 & 0 & \cdots \\ \mathbf{1} & 0 & 0 & 0 & \cdots \\ 0 & 0 & 0 & 0 & \cdots \\ \cdots & \cdots & \cdots & \cdots & \cdots \end{array} \right]_{aj} \\
&\equiv \frac{(n-1)!}{d_{R'_1}} \delta_{R'_1 S'_1} (I_{R'_1 S'_1})_{ib} (I_{S'_1 R'_1})_{aj}
\end{aligned}$$

where the form of the intertwiners has been spelled out.

Bibliography

- [1] S. Corley, A. Jevicki and S. Ramgoolam, “Exact correlators of giant gravitons from dual $N = 4$ SYM theory,” *Adv. Theor. Math. Phys.* **5**, 809 (2002) [arXiv:hep-th/0111222].
- [2] V. Balasubramanian, D. Berenstein, B. Feng and M. x. Huang, “D-branes in Yang-Mills theory and emergent gauge symmetry,” *JHEP* **0503**, 006 (2005) [arXiv:hep-th/0411205].
- [3] R. de Mello Koch, J. Smolic and M. Smolic, “Giant Gravitons - with Strings Attached (I),” *JHEP* **0706**, 074 (2007), arXiv:hep-th/0701066.
- [4] R. de Mello Koch, J. Smolic and M. Smolic, “Giant Gravitons - with Strings Attached (II),” *JHEP* **0709** 049 (2007), arXiv:hep-th/0701067.
- [5] Y. Kimura and S. Ramgoolam, “Branes, Anti-Branes and Brauer Algebras in Gauge-Gravity duality,” arXiv:0709.2158 [hep-th].
- [6] D. Bekker, R. de Mello Koch and M. Stephanou, “Giant Gravitons - with Strings Attached (III),” arXiv:0710.5372 [hep-th].
- [7] T. W. Brown, P. J. Heslop and S. Ramgoolam, “Diagonal multi-matrix correlators and BPS operators in $N=4$ SYM,” arXiv:0711.0176 [hep-th].

- [8] R. Bhattacharyya, S. Collins and R. d. M. Koch, “Exact Multi-Matrix Correlators,” *JHEP* **0803**, 044 (2008) [arXiv:0801.2061 [hep-th]].
- [9] T. W. Brown, P. J. Heslop and S. Ramgoolam, “Diagonal free field matrix correlators, global symmetries and giant gravitons,” arXiv:0806.1911 [hep-th].
- [10] Y. Kimura and S. Ramgoolam, “Enhanced symmetries of gauge theory and resolving the spectrum of local operators,” *Phys. Rev. D* **78**, 126003 (2008) [arXiv:0807.3696 [hep-th]].
- [11] Y. Kimura, “Non-holomorphic multi-matrix gauge invariant operators based on Brauer algebra,” arXiv:0910.2170 [hep-th].
- [12] S. Ramgoolam, “Schur-Weyl duality as an instrument of Gauge-String duality,” *AIP Conf. Proc.* **1031**, 255 (2008) [arXiv:0804.2764 [hep-th]].
- [13] V. Balasubramanian, M. Berkooz, A. Naqvi and M. J. Strassler, “Giant gravitons in conformal field theory,” *JHEP* **0204**, 034 (2002) [arXiv:hep-th/0107119].
- [14] G. ’t Hooft, “A Planar Diagram Theory for Strong Interactions,” *Nucl. Phys. B* **72**, 461 (1974);
G. ’t Hooft, “A Two-Dimensional Model For Mesons,” *Nucl. Phys. B* **75**, 461 (1974).
- [15] R. de Mello Koch, “Geometries from Young Diagrams,” *JHEP* **0811**, 061 (2008) [arXiv:0806.0685 [hep-th]].
- [16] R. de Mello Koch, N. Ives and M. Stephanou, “Correlators in Nontrivial Backgrounds,” *Phys. Rev. D* **79**, 026004 (2009) [arXiv:0810.4041 [hep-th]].

- [17] R. de Mello Koch, T. K. Dey, N. Ives and M. Stephanou, “Correlators Of Operators with a Large R-charge,” arXiv:0905.2273 [hep-th].
- [18] H. Lin, O. Lunin and J. M. Maldacena, “Bubbling AdS space and 1/2 BPS geometries,” JHEP **0410**, 025 (2004) [arXiv:hep-th/0409174].
- [19] V. Balasubramanian, J. de Boer, V. Jejjala and J. Simon, “The library of Babel: On the origin of gravitational thermodynamics,” JHEP **0512**, 006 (2005) [arXiv:hep-th/0508023],
V. Balasubramanian, V. Jejjala and J. Simon, “The library of Babel,” Int. J. Mod. Phys. D **14**, 2181 (2005) [arXiv:hep-th/0505123].
- [20] V. Balasubramanian, J. de Boer, V. Jejjala and J. Simon, “Entropy of near-extremal black holes in AdS₅,” JHEP **0805**, 067 (2008) [arXiv:0707.3601 [hep-th]],
R. Fareghbal, C. N. Gowdigere, A. E. Mosaffa and M. M. Sheikh-Jabbari, “Nearing Extremal Intersecting Giants and New Decoupled Sectors in N = 4 SYM,” JHEP **0808**, 070 (2008) [arXiv:0801.4457 [hep-th]].
- [21] J. M. Maldacena, “The large N limit of superconformal field theories and supergravity,” Adv. Theor. Math. Phys. **2**, 231 (1998) [Int. J. Theor. Phys. **38**, 1113 (1999)] [arXiv:hep-th/9711200];
S. S. Gubser, I. R. Klebanov and A. M. Polyakov, “Gauge theory correlators from non-critical string theory,” Phys. Lett. B **428**, 105 (1998) [arXiv:hep-th/9802109];
E. Witten, “Anti-de Sitter space and holography,” Adv. Theor. Math. Phys. **2**, 253 (1998) [arXiv:hep-th/9802150].
- [22] K. Skenderis and M. Taylor, “Anatomy of bubbling solutions,” JHEP **0709**, 019 (2007) [arXiv:0706.0216 [hep-th]].

- [23] D. E. Berenstein, J. M. Maldacena and H. S. Nastase, “Strings in flat space and pp waves from $N = 4$ super Yang Mills,” *JHEP* **0204**, 013 (2002) [arXiv:hep-th/0202021].
- [24] H. Y. Chen, D. H. Correa and G. A. Silva, “Geometry and topology of bubble solutions from gauge theory,” *Phys. Rev. D* **76**, 026003 (2007) [arXiv:hep-th/0703068].
- [25] R. de Mello Koch, T. K. Dey, N. Ives and M. Stephanou, “Hints of Integrability Beyond the Planar Limit,” *JHEP* **1001**, 014 (2010) [arXiv:0911.0967 [hep-th]].
- [26] H. Lin, A. Morisse and J. P. Shock, “Strings on Bubbling Geometries,” *JHEP* **1006**, 055 (2010) [arXiv:1003.4190 [hep-th]].
- [27] H. Lin, “Studies on 1/4 BPS and 1/8 BPS geometries,” arXiv:1008.5307 [hep-th].
- [28] J. McGreevy, L. Susskind and N. Toumbas, “Invasion of the giant gravitons from anti-de Sitter space,” *JHEP* **0006**, 008 (2000) [arXiv:hep-th/0003075];
M. T. Grisaru, R. C. Myers and O. Tafjord, “SUSY and Goliath,” *JHEP* **0008**, 040 (2000) [arXiv:hep-th/0008015];
A. Hashimoto, S. Hirano and N. Itzhaki, “Large branes in AdS and their field theory dual,” *JHEP* **0008**, 051 (2000) [arXiv:hep-th/0008016].
- [29] D. Berenstein, “A toy model for the AdS/CFT correspondence,” *JHEP* **0407**, 018 (2004) [arXiv:hep-th/0403110].
- [30] R. d. M. Koch, G. Mashile and N. Park, “Emergent Threebrane Lattices,” *Phys. Rev. D* **81**, 106009 (2010) [arXiv:1004.1108 [hep-th]].

- [31] A. Mikhailov, “Giant gravitons from holomorphic surfaces,” JHEP **0011**, 027 (2000) [arXiv:hep-th/0010206].
- [32] C. E. Beasley, “BPS branes from baryons,” JHEP **0211**, 015 (2002) [arXiv:hep-th/0207125].
- [33] J. Kinney, J. M. Maldacena, S. Minwalla and S. Raju, “An index for 4 dimensional super conformal theories,” Commun. Math. Phys. **275**, 209 (2007) [arXiv:hep-th/0510251].
- [34] I. Biswas, D. Gaiotto, S. Lahiri and S. Minwalla, “Supersymmetric states of $N = 4$ Yang-Mills from giant gravitons,” JHEP **0712**, 006 (2007) [arXiv:hep-th/0606087].
- [35] G. Mandal and N. V. Suryanarayana, “Counting 1/8-BPS dual-giants,” JHEP **0703**, 031 (2007) [arXiv:hep-th/0606088].
- [36] J. Pasukonis and S. Ramgoolam, “From counting to construction of BPS states in $N=4$ SYM,” arXiv:1010.1683 [hep-th].
- [37] V. Balasubramanian, M. x. Huang, T. S. Levi and A. Naqvi, “Open strings from $N = 4$ super Yang-Mills,” JHEP **0208**, 037 (2002) [arXiv:hep-th/0204196],
O. Aharony, Y.E. Antebi, M. Berkooz and R. Fishman, “Holey sheets: Pfaffians and subdeterminants as D-brane operators in large N gauge theories,” JHEP **0212**, 096 (2002) [arXiv:hep-th/0211152].
- [38] D. Sadri and M. M. Sheikh-Jabbari, “Giant hedge-hogs: Spikes on giant gravitons,” Nucl. Phys. B **687**, 161 (2004) [arXiv:hep-th/0312155].
- [39] D. Berenstein, “Shape and holography: Studies of dual operators to giant gravitons,” Nucl. Phys. B **675**, 179 (2003) [arXiv:hep-th/0306090].

- [40] D. Berenstein, D. H. Correa and S. E. Vazquez, “A study of open strings ending on giant gravitons, spin chains and integrability,” [arXiv:hep-th/0604123],
D. Berenstein and S. E. Vazquez, “Integrable open spin chains from giant gravitons,” JHEP **0506**, 059 (2005) [arXiv:hep-th/0501078],
D. Berenstein, D. H. Correa and S. E. Vazquez, “Quantizing open spin chains with variable length: An example from giant gravitons,” Phys. Rev. Lett. **95**, 191601 (2005) [arXiv:hep-th/0502172],
D. H. Correa and G. A. Silva, “Dilatation operator and the Super Yang-Mills duals of open strings on AdS Giant Gravitons,” [arXiv:hep-th/0608128].
- [41] Y. Kimura, “Quarter BPS classified by Brauer algebra,” JHEP **1005**, 103 (2010) [arXiv:1002.2424 [hep-th]].
- [42] E. D’Hoker and A. V. Ryzhov, “Three-point functions of quarter BPS operators in $N = 4$ SYM,” JHEP **0202**, 047 (2002) [arXiv:hep-th/0109065],
E. D’Hoker, P. Heslop, P. Howe and A. V. Ryzhov, “Systematics of quarter BPS operators in $N = 4$ SYM,” JHEP **0304**, 038 (2003) [arXiv:hep-th/0301104],
P. J. Heslop and P. S. Howe, “OPEs and 3-point correlators of protected operators in $N = 4$ SYM,” Nucl. Phys. B **626**, 265 (2002) [arXiv:hep-th/0107212].
- [43] T. W. Brown, “Permutations and the Loop,” arXiv:0801.2094 [hep-th].
- [44] T. W. Brown, “Cut-and-join operators and $N=4$ super Yang-Mills,” arXiv:1002.2099 [hep-th].

- [45] N. Beisert, C. Kristjansen and M. Staudacher, “The dilatation operator of $N = 4$ super Yang-Mills theory,” Nucl. Phys. B **664**, 131 (2003) [arXiv:hep-th/0303060].
- [46] R. de Mello Koch and R. Gwyn, “Giant graviton correlators from dual $SU(N)$ super Yang-Mills theory,” JHEP **0411**, 081 (2004) [arXiv:hep-th/0410236].
- [47] R. Bhattacharyya, R. de Mello Koch and M. Stephanou, “Exact Multi-Restricted Schur Polynomial Correlators,” arXiv:0805.3025 [hep-th].
- [48] S. R. Das, A. Jevicki and S. D. Mathur, “Vibration modes of giant gravitons,” Phys. Rev. D **63**, 024013 (2001) [arXiv:hep-th/0009019].
- [49] R. C. Meyers, “Dielectric-branes,” JHEP **9912**, 022 (1999) [arXiv:hep-th/9910053].
- [50] W. Carlson, R. de Mello Koch and H. Lin, work in progress.
- [51] L. Susskind, “*The Black Hole War*,” New York, Back Bay Books, (2009).
- [52] J. Maldacena, “The Large N limit of supersymmetric field theories and supergravity,” Adv. Theor. Math. Phys 2:231, (1998), [arXiv:hep-th/9711200].
- [53] G. 't Hooft, “Dimensional reduction in quantum gravity,” [arXiv:hep-th/9310026].
- [54] L. Susskind, “The World as a Hologram,” (1995), [arXiv:hep-th/9409089].

- [55] J. L. Petersen, “Introduction to the Maldacena Conjecture on AdS/CFT,” (1999), [arXiv:hep-th/9902131v2].
- [56] E. D’Hoker, D. Z. Freedman, “Supersymmetric Gauge Theories and the AdS/CFT Correspondence,” (2002), [arXiv:hep-th/0201253v2].
- [57] M. E. Peskin, D. V. Schroeder, “An Introduction to Quantum Field Theory,” United States Of America, Westview Press, (1995).